We thank the reviewers for the constructive reviews and suggestions. The comments by the reviewers are in indented blocks and italic fonts. Our response follows each comment and changes in the manuscript are – if shortly- written here in quotation marks.

Reviewer 1

> T*his paper forces a 1d coupled glacier-plume model with future climate from the CMIP5 climate models to project the future behavior of 12 of Greenland's tidewater glaciers. The topic of sea level rise and ice-ocean interactions in Greenland is of great contemporary interest, and the use of a plume model is certainly an improvement (subject to concerns about tuning and true representation of coupling between melting and calving) on previous similar studies such as Nick et al. 2013.*
>
> *Overall I think it is easy to criticize papers doing future projections because there are a great many factors to consider and decisions to be made, and many compromises are necessary. I have tried to write my review with this in mind, and I commend the authors for bringing many datasets and models together and for addressing the many challenges inherent in projecting future sea level from Greenland. Contrary to the previous reviewers I did not find the paper to be clearly written; perhaps it is simply the nature of describing a complex model with many inputs, but I found several passages to be rather hard to follow (notably the ocean forcing description), which will also come across in my review.*

We understand that the complexity of Model inputs can be confusing and we therefore now introduced Figure 2, which shows an overview and the interaction of all the different model components. A short summary on the the data input introduces the subsection in section 3.

> *I do have some major concerns, some of which might be misunderstandings arising from a lack of clarity, but these should be addressed or the writing improved. For example, I am concerned there may be some important errors with the surface mass balance. On the use of a flowline model, I agree with the previous reviewers that this is a serious limitation and the field is beginning to move beyond flowline models. On balance however, I do not think this should preclude publication provided this is clearly acknowledged, the paper focuses more on the main qualitative points of interest and the major comments below can be addressed.*

As we will explain in the major comment section, we do not see any "important errors" in our calculations of the surface mass balance. We are aware that some workers do "move beyond flowline models" but this doesn't make flowline models irrelevant. The modeling of such a complex and nonlinear system as the Greenland glacier system, it is natural to use different modeling approaches (spectrum of models) which are useful to address different aspects of the problem.

> *For me, the two strongest points this paper makes are (i) that when upscaling results from a handful of glaciers to the whole ice sheet we should be careful about which and how many glaciers we sample, and (ii) quantifying the importance of dynamics-SMB coupling in future projections, though I found the discussion and figures on this point to be highly confusing. In general I felt the paper could benefit from focusing on/emphasizing/clarifying these points.*
> *I have split my comments in major and minor comments. I have not noted every spelling and grammatical error as these are rather numerous and should be easy to spot.*

Major comments

> *1. Representation of melting and the coupling of melting to calving*
> *A plume model is used to represent submarine melting of the calving front. When a floating tongue is present, this is naturally applied as a thinning of the tongue. When the glacier has no floating portion the submarine melting is applied as a thinning of the last grounded cell, which is less natural (it is essentially treating the submarine melting as a surface mass balance). Calving is represented via the commonly used crevasse depth criterion. My major comment is: how do we know that this treatment of combined melting/calving actually captures the effect of submarine melting on calving? How does it relate to emerging understanding of the coupling between melting and calving through undercutting (e.g. Benn et al. 2017, J. Glac.)?*
> *For calving fronts without a floating portion, how well does the application of submarine melting as a 'vertical' surface mass balance term represent the 'truer' process of melting incising horizontally into the calving front?*

At the moment it feels as though the authors have taken their approach because it is the one which works for their model rather than on the basis of representation of processes. Reaching the conclusions of this paper without discussing at all whether the model actually captures ice-ocean processes seems remiss. I see that this is very briefly mentioned in the discussion and conclusions sections but this is too little and too late at the moment.

a) **Treatment of submarine melt in the model**. It only seems "natural" to treat lateral submarine melt as the flux in the equation for ice thickness (Eq. 1). In fact, as any gridded ice sheet model (including 3-D models), our flowline model has only one characteristics for ice distribution – ice thickness and therefore submarine melt can only appear in the equation for ice thickness. However, in the case of an absence of floating tongue, changes in the thickness of the last grid cell is immediately recalculate to the change of the position of grounding line. As a result, our grounding line respond to changes in submarine melt in continuous and realistic manner but, of course, neglects undercutting (see the next section).

b) **Undercutting**. We are aware about recent studies on the effects of submarine melting on calving processes, but these studies are still limited by several types of calving styles and the high resolution models used in (Benn et al. 2017, J. Glac.) cannot be applied to realistic conditions. Undercutting can amplify calving but can also stabilize glaciers. Benn et al. (2017, J. Glac) presume that there is a rather "small effect of under-cutting on glacier stability " in Greenland. Undercutting is not included in our simulations because it cannot be explicitly described in 1-D model and appropriate parameterization for this processes does not exist yet. However, the large uncertainties of the calving processes are included implicitly in our parameter β . Of course, undercutting is not the only process which is still poorly understood and not included in our simulations. However we strongly disagree with the reviewer's statement that we chose our approach "*because it is the one which works for their model rather than on the basis of representation of processes*". We used a rather standard modeling approach which has been used in numerous previous studies but add one improvement – explicit treatment of submarine melt throug h turbulent plume parameterization. Our result clearly show that this is an important improvement.

2. Tuning of model
In order to initialize the model to obtain glaciers close to their present day state, the authors first vary 4 key parameters with a fixed (non-plume) melt rate and find a combination of these parameters which puts the glacier close to its present day state. They then turn on the plume model and tune 2 key parameters to maintain the glacier close to present day. The resulting set of parameters is used for the future simulations.Overall, I have two main issues. First, do you know that the values of the first 4 parameters are the only values which would work? It is not at all obvious that there should be 1 unique set of parameters which work. This is important because a different set of parameters might lead to a different evolution in the future.

The four parameters determining glaciers dynamics have been selected by minimizing errors in accurately measured ice thickness and discharge through the grounding line. Of course, the selection of a single model performance metric to some extent is subjective, but as soon as this metric is selected, the values of four parameters are uniquely defined unless completely different combinations of these four parameters produce precisely the same value of the performance metric which is extremely unlikely. Thus the answer to the the first reviewer's question is " other combinations of these parameters also will work but not as good as the set we used. Since our aim was to investigate the effect of global warming on the future glacier dynamics and mass loss, we chose to only vary two parameters - *β* and *fwd* – which control submarine melt and calving. Already variations of these two parameterrs lead to large uncertainty ranges. Introducing even more uncertain parameters would would reduce the readability of the paper.

Second, I am uncomfortable with how much the parameters vary from glacier to glacier (by two orders of magnitude in some cases); one would hope that if the model has a good representation of the physics then the parameters should take reasonably close values between glaciers.

In fact, most of the parameters that determine the glacier flow are in the same order of magnitude for different glaciers. The only notable exception is the high width-scaling parameter W_s (enhances lateral stress) for Store glacier and comes from the fact that Store glacier is a fast-flowing glacier situated to the top of a sill (Fig. S9), that makes this glacier unstable unless there are high lateral stresses acting to stabilize it. The great variance of the sliding factor A_s between different glaciers is not surprising and has been shown recently by Stearns and van der Veen (2018, Science)

Once more this leads me to question how robust the future projections are. For example, it might be that due to uncertainties in other aspects of the model (e.g. bed topography), you have to tune up *the melt rate a lot to match the glacier in the present day (high value of beta). But then presumably you are hard-wiring that glacier to be highly sensitive to ocean warming and prejudicing its future evolution. I am not convinced that this is physical rather than just an artifact of the initialization and missing model physics or poor input data.*

There are always uncertainties in model physics and input data that will influence the numerical experiments. However, we do not hardwire our glacier model to be more sensitive to submarine melting, since we always vary β from 0.3 to 3. (see Table S3).

3. Clarity of description – notably ocean forcing
I found certain aspects of the description of the model and its inputs rather confusing - in general I think the paper would be much improved if the description of the model and inputs could be clarified and simplified.

The most confusing part for me at the moment is the fjord temperature and salinity profiles. If I understand correctly, you use either the CTD profiles or the reanalysis data for the spin-up, and then you add the CMIP5 trends on top of the spin-up period to do the future projections. If this is the case it needs to be made clearer. It also wasn't clear to me when the CTD data was used and when the reanalysis data was used. There is a long discussion of how the CTD data and reanalysis data differ, but ultimately this discussion comes to nothing because you use both anyway. This is one example of how this paper could be a lot more readable – perhaps move the detailed discussion comparing CTD and reanalysis to the supplement, allowing you to focus on describing what actually goes into the model. It would be great if you could provide an equivalent to equation 17 for the fjord temperature – this would really help the reader understand what is being done.

We agree with the reviewer and moved the part on how the TS profiles were constructed to the supporting information. Equation 19 now describes the future ocean temperature forcing. Furthermore we now inserted a new figure (Fig. 2) that gives an overview off all the input data used for the future scenarios. A short summary of all the input data is given in section 3.:

"To simulate the response of the glacier-plume model to future global warming we considered the potential changes of surface mass balance (SMB) and submarine melting. To this end, for each glacier, we derived data sets for three forcing factors from the year 2000 till 2100: spatially distributed SMB (section 3.3), subglacial discharge (section 3.3) and fjord water temperatures (section 3.4).
For changes in SMB we used anomalies from the simulation with the regional climate model MAR, forced by global GCM MIROC for the RCP8.5 scenario. In our previous study (Calov et al., 2018) we used the same SMB changes toforce the 3D ice-sheet model SICOPOLIS . Now we use results of this simulation to compute the subglacial discharge for each glacier from simulated surface runoff . Changes in ocean temperature were included by applying a linear warming trend, derived from several different CMIP5 models. On every time step the three forcing factors where provided as data-input and forced the glacier-plume model (Fig. 2). While for each glacier the future evolution of the subglacial discharge and ocean temperature where firmly prescribed in the data-sets, the SMB-input was interactively corrected for the surface elevation feedback and thus considered the glacier surface height on each time step. The upcoming subsections describe the choice of glaciers, how the geometry for the 1D model was derived and how the corresponding forcing factors were determined and applied."

4. Use of CMIP models
The authors use 1 CMIP model for the surface mass balance (or in fact a regional climate model forced by the CMIP model) and 3 CMIP models for the ocean forcing. This disparity has been commented on by the other reviews and I am not convinced by the authors' response. As the authors themselves state in their response to previous reviews, "climate change scenarios (both in terms of GHGs concentration and model output) are the major source of uncertainties." This makes it sound like you might have reached different conclusions if you had used different CMIP models – can you be sure that your conclusions are independent of the CMIP models or that the CMIP models you have used are in some way representative of others?

Indeed we used a single climate change scenario simulated with the regional climate model MAR forced by output of the MIROC5 model for the RCP8.5 concentration scenario, the same as we used in Calov et al. (2018). The choice of MAR-MIROC5 scenario is justified by the fact that it is medium in terms of Greenland SMB change compare to the results for other GCMs (see fig.3 in Calov et al., 2018). Of course, it would be useful to perform similar study with other climate change scenarios but it is important to realized that generating of each scenario is extremely computationally and time-demanding procedure involving several authors of the paper. The first stage of this procedure was acquiring regional model output, interpolated it to SICOPOLIS ice sheet grid and calculating several parameters needed for elevation correction of SMB, surface air temperature and surface runoff for each year and for each model grid cell. At the second stage, the SICOPOLIS model has been run for 100 years forced by the SMB anomalies. The output of this experiment - annually averaged elevation corrected surface runoff, basal melt rate and elevation - were used during the third stage using to force the basal hydrology model HYDRO to calculate monthly subglacial discharge for each year and for each glacier. Finally, SMB and elevation corrected coefficients from the regular ice sheet model grid were interpolated to the central lines of each glacier and, together with simulated subglacial discharge, used to drive the glacier-plume model. Obviously, for each new scenario, all these stages have to be repeated. Although we performed simulations only with one climate scenario (but for a range of ocean warming scenarios), we see no reason why we would arrive to a different conclusion if we would use another GCMs. Of course, the numbers for SLR are scenario-dependent but the main conclusion of our paper that changes in submarine melt due to ocean warming and increased subglacial discharge are the dominant factor determining the contribution of Greenald glaciers to SLR and that this contribution is comparable with mass losses from the rest of GrIS are robust.

5. Upscaling of SLR
I think the discussion on scaling up of sea level rise from a handful of glaciers to the whole ice sheet is very interesting and important. I wonder if this could be emphasized more in the paper by bringing supplementary figure 7 into the main paper and expanding the discussion? For a direct comparison to Nick et al. 2013, could you do the linear regression with the same 4 glaciers as in their paper?

We agree and moved Figure S7 into the manuscript (Now, Figure 13). We also added discussion of the sensitivity of the upscaling method.
Unfortunately, the selection of glaciers from Nick et al. 2013 includes Petermann glacier, which we did not chose in our selection since we showed in Beckmann et al. (2018a) that simulated with the plume model submarine melt for Peterman glacier did not show good agreement with the obserservation, since the Coriolis force is not considered in the plume model and for very long floating tongue of Petermann glacier this is serious omission

6. Surface mass balance
*I am a little surprised about how small the surface mass balance contribution is without dynamics (Fig. 11, brown). According to Fettweis et al 2013, MAR forced by MIROC5 results in SLR of 9.2 cm by 2100 due to surface mass balance alone. I appreciate this is for the whole ice sheet, but your 12 glaciers probably cover ~5% of the ice sheet area and therefore I would expect a rough SMB-only SLR of 0.05*92 mm = 4.5 mm from your glaciers which is much larger than your brown shading. Why is this? Possibly I am getting confused about your separation in Fig. 11 – what is the difference between the orange and brown shading? Could you clarify this in the text as well? For example, you say "that the SMB-forcing alone derived from MAR (without the glacier's response) has an almost negligible effect on SLR (Fig. 11 b, brown curve)" – how can this be the case when MAR projects 9.2 cm of SLR for the whole ice sheet when forced by MIROC5 (Fettweis et al. 2013)?*

We doubled checked our numbers and come to the same result as before. The 9cm from Fettweis come from the whole ice sheet. Our glacier cathment area (see fig. 3) however is not evenly partitioned between accumulation zone and ablation zone with the accumulation zone absolutely dominates (Imagine a triangle, where only the tip belongs to the ablation zone and the rest of the triangle belongs to the accumulation zone). Thus a net surface mass loss is rather small since it is only controlled by the (much smaller) ablation area which is less than 5 %. If we want to compare with Fettweis here, we could probably compare the sum of the width of all the 12 glacier termini (55 km) to the length of the Greenland coast line(44 000 km). This gives us a fraction of 0.1%. which in turn would correspondd only 0.1mm SLR.

Page 15, lines 16-18, Fig. 15 and Fig S1: Similarly, I find it hard to believe that the SMB contribution to sea level is negative for some glaciers under an RCP 8.5 scenario (e.g. Rink – Fig. 15). Looking at SMB anomalies by 2100 in MAR forced by MIROC5 (Fettweis et al. 2013, Fig. 5, bottom left panel), it certainly doesn't look like any glacier would have an increasingly positive surface mass balance and it doesn't look like there is any reason for Rink to be very different than Store (which is nearby), as is implied by Fig. 15. Can you check these numbers?

Rink glacier has no negative contribution to SLR, it is about 0 in our experiment. We added a zero-line in the plot now and corrected in the text. It is true, that Rink and Store glacier a similar SMB forcing (see Figure S1, equivalent to less than 0.05 mm SLR) but Fig. 15 here shows the dynamic response of the glacier to the SMB forcing and it is very different for these two glaciers. Therefore it is important where the forcing acts (close to termini) and how e.g. the underlying bedrock forms the dynamic response of the glacier: As seen in the new Figure 6, Store glacier is located on the tip of a sill and a small negative SMB forcing at the glacier termini is sufficient to push Store glacier on the steep retrograde bed which leads its strong retreat whereas Rink glacier is rather stable. We thank the reviewer for this question, since it shows the importance of the dynamics response and we therefore put this example into the text.

A second comment: you say in the introduction that you neglect the effect of ice sheet boundary retreat on subglacial discharge. Do you also neglect the effect of ice sheet boundary retreat on SLR from surface mass balance? In other words, are you still summing up the surface mass balance contribution to sea level from areas where the ice sheet has retreated (e.g. the 30 km over which Jakobshavn is projected to retreat). If so, presumably you might be substantially overestimating the contribution to sea level from SMB?

We think our sentences were maybe a bit confusing in this part about the subglacial discharge.
The phrase 'neglecting ice sheet boundary retreat' was unfortunate and referred to a pure technicality on the allocation procedure of the subglacial discharge for each glacier.
In our future scenarios when simulating subglacial discharge we accounted for changes in surface runoff, basal melt, and ice sheet retreat since it was determined by simulations with Sicopolis (Calov et al 2018). At the beginning of the simulations we determined the boundary gird cells of the present-day ice mask that belong to each fjord and glacier. Thus the discharge out of this ice-mask cells (to which the subglacial discharge is routed) determines the discharge into the fjord. This 'routing end-points' for each glacier were held constant over future simulations . Thus the present-day ice mask was used only for the routing and allocation of the subglacial discharge.

All our experiment of the glacier, show the dynamic response, where glacier retreat (and ice sheet retreat)is of course considered. Since this phrasing of 'neglecting the ice sheet boundary effect' lead to so much confusion we deleted it aiming for more clarity in the paper.

In general I was quite confused by how you are splitting up the different components of sea level - could you make this very clear (e.g. particularly the difference between the brown and orange shadings in Fig. 11)?

The height of the brown area represents the "static SMB effect" which is computed as e cumulative integral of SMB anomaly from MAR over a constant cathement area and constant (present-day) elevation of all 12 glaciers . The height of theof yellow area shows the additional SLR contribution from responding glacier dynamics, namely changes in velocity caused by changes in glaciers elevation caused by SMB changes (but without effect of elevation changes on SMB). At last the height of the orange area represents an additional effect of elevation correction on SMB. Thus comparison of brown, yellow and orange areas clearly show that the main effect of SMB on glaciers mas loss occurs indirectly, through the changes in glaciers dynamics (velocities) which is not a trivial result. The red area represent adding effect of temperature change and blue area –adding effect of subglacial discharge change. Note, that this is not classical factor analysis where the effect of different factors are investigated separately. Here we add factors sequentially to illustrate the importance of all three factors – SMB, ocean temperature and subglacial discharge.
To clarify rewrote the whole part:

"When forced by comprehensive climate change scenarios (changes in SMB with the surface elevation feedback, ocean temperature T and subglacial discharge Q) the median estimate for SLR contribution from all 12 glaciers is about 18 mm (17.9 mm) at the year 2100 (Fig. 8 a, and Fig. 8 b, blue curve). To quantify the role of the individual forcing factors, we performed an additional set of simulations with the same model versions corresponding to the median SLR response (18mm) but applying the three different forcing factors in sequence. With the same model version we rerun for each glacier the experiment omitting changes in subglacial discharge (denoted "SMB + T" in Fig. 8 b, pink curve) and omitting changes in subglacial discharge and ocean temperatures (denoted "SMB" in Fig. 8 b, sum of the brown, orange and yellow areas). The total effect of SMB change on SLR is decomposed into "static" (brown), "dynamic" (yellow) and effect of elevation correction (orange). "Static" effect was computed as the cumulative integral of SMB anomalies over the fixed present-day catchment and elevation of individual glaciers. As Fig. 8b shows, this component is close to zero which is explained by the geometry of the glaciers' catchment area, where the ablation area is

much smaller than accumulation area. For some glaciers, the cumulative SMB over the glacier's catchment even increased towards the end of 21 century due to increased precipitation over accumulation area (Fig S1, supporting information). Thus most of SLR due to SMB change alone occur through the dynamical processes – thinning and acceleration of glaciers, which in turn affects the calving rate. The surface elevation feedback (Fig. 8 b, yellow curve). has only a minor effect on the glaciers response to SMB change which is not the case for the entire GrIS (Calov et al., 2018) where this effect is important.
As explained above, we attribute 30 % of the 18mm SLR to the response to changes in SMB alone. The remaining 70 % of SLR is thus caused by the response toocean warming and increased subglacial discharge (Fig. 8 b, blue and pink area together). We found that both factors, ocean warming and increased subglacial discharge, are of comparable importance for SLR (by comparing the blue and pink curve in Fig. 8 b These estimates are valid only for the cumulative SLR of all 12 glaciers. Each individual glacier may respond differently to the individual forcing factors. For instance, Kong-Oscar Glacier (Fig. 9) is slightly gaining mass with the SMB forcing alone and shows a retreat by 10 km and contribution 1 mm to SLR due to ocean warming. When the increase in subglacial discharge is added to the ocean warming, the glacier retreats another 10 km and contributes additionally 2 mm to SLR.

Minor comments

Page 1 line 19: you indicate that 70% of SLR is associated with a response to increased submarine melting. Could you clarify here and throughout the paper exactly what is meant by this? Is it that increased calving and submarine melting alone are accounting for 70% of SLR, or is it that increased calving and submarine melting together with decreased SMB due to dynamic thinning are accounting for 70%? This is an important distinction – the latter possibility would include a dynamics-SMB coupling whereas the former is pure dynamics.

The reviewer's question is right to the point. In fact, we do not attribute 70% of SLR to increased submarine melting and 30% to increased surface melt. What we derived from our experiments is that changes in SMB alone (with constant ocean temperature T and subglacial discharge Q can only explain 30% of SLR simulated in the experiments where all three factors were taken into account. Therefore remaining 70 % are attributed to the glaciers response to changes in ocean temperature and Q. These two factors, assuming all other are kept constant, do cause increased submarine melt. However, in the transient experiments, there is a complex interplay between all three processes (surface and submarine melt, and calving). This is why in the revised manuscript we changed "changes in submarine melt" to "change in ocean temperature and subglacial discharge which control the submarine melt".

Page 3 line 28: you have assessed the uncertainty for calving and melting parameters (at least for a single calving law) but in relation to climate scenarios you have only considered RCP8.5 and a single CMIP model on the SMB side – so I think you have not really quantified uncertainty related to climate change scenarios and maybe this statement should be removed.

Agreed, we deleted the words climate scenarios and only refer to the proportion of calving and submarine melting and ocean warming.

Page 5 line 10: 'initial boundary condition' – it would be clearer if you changed this to the 'boundary condition at the ice divide' or 'boundary condition at the top of the glacier catchment'.

Agreed,done.

Section 2.2: it would be good to acknowledge briefly the extent to which this plume model approach captures what is known about submarine melting. E.g. it does capture vertical variability in melt rate within a plume (Jenkins 2011), but it can't capture variability across the calving front due to presence/absence of plumes (Fried et al. 2015), and it can't capture melting outside of plumes due to melt-driven convection (Magorrian & Wells, 2016) or fjord-wide circulation (Slater et al. 2018).

The plume actually simulate melt-driven convection if the subglacial discharge is small (Beckmann et al. 2018) but of course-as the reviewers mentions- not outside the plume. In the nature of a width-averaged 1D plume is of course it's limit in terms of variability across the calving front. We added now: "The plume is a 1D model and therefore can neither simulate variability across the calving front (Fried et al., 2015), nor account for fjord wide circulation (Slater and Straneo, 2018) across and outside plumes. However, the width-averaged melt rates - as only required for the 1d glacier model- can be simulated with the 1D plume model (Beckmann et al., 2018)."

Section 2.3: it might improve the readability of the paper if some of these technical details which are not central to the main messages of the paper (e.g. the definition of the total submarine melting) could be moved to supporting information – just a suggestion so feel free to ignore.

We left this description in the main part, this this is the essential part of the glacier-plume model. And reviewers before have ask for the detailed equations e.g. the plume.

Page 16 line 15: pvalue=0 is a bit meaningless – better to say p<0.01 or similar.

Done.

Page 18 line 19: I think it would be more natural to state the proportion of SLR which is attributable to dynamics (i.e. the dynamical response of Greenland's outlet glaciers can account for 5/13.8 = 36% of total sea level contribution from the Greenland ice sheet).

This is not correct. 5 cm of SLR which we obtained by upscaling of dynamical glacier response is not a part of 13.8 cm SLR simulated in Calov et al. 2018 but additional SLR not accounted in Calov et al. (2018).

Table 2: some of the column headings have a 'Delta' symbol in them which are not mentioned in the figure caption – are they meant to be there?

We thank the reviewer for spotting this mistake. We deleted the Delta symbol, such that the caption entry corresponds to the table heading.

Figure S2 – you say here you used Bedmachinev3 topography but in the main article you state you used Bedmachinev2 (page 8 line 18). Which was it?

Yes we used Bedmhachinev2 throughout our experiments as described in the main text. We had started with our experimental setup when there wasn't the newest Bedmachinev3 available. This Figure only illustrates the sill depth determination with the best available data set (now, Fig. S8) to show the potential effect of the bathymetry on the reconstructed temperature profiles from reanalysis data (Fig. S3). Therefore we use Bedmachinev3, which contains the latest data on fjord bathymetry. We show that considering this sill (with the best available data) would shift the reanalysis temperature profile even further apart from the measurement close to the glacier and therefore does not improve the reconstruction of temperature profiles from reanalysis data sets. Thus our current method (deriving the temperature profile from the 400m-depth point) is an adequate approach. We add this part in the caption of the Figure (now Figure S8)

Supplement – please improve figure captions throughout – at the moment they are sloppy. For example Fig S4 – annual subglacial discharge from what? Fig S5 has two missing references.

Done.

References which are not in the paper

Fried, M. J., Catania, G. A., Bartholomaus, T. C., Duncan, D., Davis, M., Stearns, L. A., et al. (2015). Distributed subglacial discharge drives significant submarine melt at a Greenland tidewater glacier. Geophysical Research Letters, 42, 9328–9336. https://doi.org/10.1002/2015GL065806

Magorrian, S. J., & Wells, A. J. (2016). Turbulent plumes from a glacier terminus melting in a stratified ocean. Journal of Geophysical Research: Oceans, 121, 4670–4696. https://doi.org/10.1002/2015JC011160

Slater, D. A., Straneo, F., Das, S. B., Richards, C. G., Wagner, T. J. W., & Nienow, P. W. (2018). Localized plumes drive front-wide ocean melting of a Greenlandic tidewater glacier. Geophysical Research Letters, 45. https://doi.org/10.1029/2018GL080763

Stearns and Van der Veen (2018): Friction at the bed does not control fast glacier flow. Science,361. DOI: 10.1126/science.aat2217

Reviewer 2

Minor technical corrections:

page 3, line 18: change "For" to "for"

Done.

page 7, line 15: there is a "dot" before "This"

Since there is a comma after the equation (15), we believe the “dot” is correct, since it signifies the end of the sentence.

page 7, line 20: there is a "dot" before "If"

Agreed, done.

page 8, line 14: "Goeltzer (2013) should have brackets

Agreed, done.

page 10/11, line 31: from 1000 to 3000 m or 1000 and 3000 m?

To be accurate we listed now all available depths of the data set: “It covers the time span from 1991--2013 with a spatial resolution of 12.5 km and for depths of 5, 30, 50, 100, 200, 400, 700, 1000, 1500, 2000, 2500, 3000 m.

Modeling the response of Greenland outlet glaciers to global warming using a coupled flowline-plume model

Johanna Beckmann[1], Mahé Perrette[1], Sebastian Beyer[1,2], Reinhard Calov[1], Matteo Willeit[1], and Andrey Ganopolski[1]

[1] Potsdam Institute for Climate Impact Research, 14412 Potsdam, Germany
[2] Alfred Wegner Institute, 27570 Bremerhaven, Germany

Correspondence: Johanna Beckmann (beckmann@pik-potsdam.de)

Abstract.

In recent decades, the Greenland Ice Sheet has experienced an accelerated mass loss, contributing to approximately 25 % of contemporary sea level rise (SLR). This mass loss is caused by increased surface melt over a large area of the ice sheet and by the thinning, retreat and acceleration of numerous Greenland outlet glaciers. The latter is likely connected to enhanced submarine melting that, in turn, can be explained by ocean warming and enhanced subglacial discharge. The mechanisms involved in submarine melting are not yet fully understood and are only simplistically incorporated in some models of the Greenland Ice Sheet. Here, we investigate the response of twelve representative Greenland outlet glaciers to atmospheric and oceanic warming using a coupled line-plume glacier-flowline model resolving one horizontal dimension. The model parameters have been tuned for individual outlet glaciers using present-day observational constraints. We then run the model from present to the year 2100, forcing the model with changes in surface mass balance and surface runoff from simulations with a regional climate model for the RCP 8.5 scenario, and applying a linear ocean temperature warming with different rates of changes representing uncertainties in the CMIP5 model experiments for the same climate change scenario. We also use different initial temperature-salinity profiles obtained from direct measurements and from ocean reanalysis data. Using different combinations of submarine melting and calving parameters that reproduce the present-day state of the glaciers, we estimate uncertainties in the contribution to global ~~sea level rise~~ SLR for individual glaciers. We also perform a sensitivity analysis of the three forcing-factors ~~, which shows that the role of different forcing (change~~ (changes in surface mass balance, ocean temperature and subglacial discharge), which shows that the role of the different forcing-factors are diverse for individual glaciers. We find that changes in ocean temperature and subglacial discharge are of comparable importance for the cumulative contribution of all twelve glaciers to global ~~sea level rise~~ SLR in the 21st century. The median range of the cumulative contribution to the global ~~sea level rise~~ SLR for all twelve glaciers is about ~~17 mm from which~~ 18 mm (the glaciers' dynamic response to changes of all three forcing-factors). Neglecting changes in ocean temperature and subglacial discharge (which control submarine melt) and investigating the response to changes in surface mass balance only leads to a cumulative contribution of 5 mm SLR. Thus, from the 18 mm we associate roughly 70 % ~~are associated with the~~ to the glaciers' dynamic response to increased ~~submarine melting~~ subglacial discharge and ocean temperature and the remaining ~~part to~~ 30% (5 mm) to the response in increased surface mass loss. We also find a strong correlation (correlation coefficient ~~0.75~~0.74) between present-day grounding line discharge

and their future contribution to ~~sea level rise~~ SLR in 2100. If the contribution of the twelve glaciers is scaled up to the total present-day discharge of Greenland, we estimate the mid-range contribution of all Greenland glaciers to 21st-century ~~sea level rise~~ SLR to be approximately 50mm. This number adds to SLR derived from a stand-alone ~~, coarse resolution~~ ice sheet model (880 mm), that does not resolve outlet glaciers and thus increases SLR by over 50 %. This result confirms earlier studies that the response of the outlet glaciers to global warming has to be taken into account to correctly assess the total contribution of Greenland to sea level change.

1 Introduction

Sea level rise (SLR) is one of the major threats to humanity under global warming, and approximately one-fourth of the recent SLR can be attributed to the Greenland Ice Sheet (GrIS) (Chen et al., 2017). In the future projections of SLR, the GrIS is not only one of the major potential contributors but also a significant source of uncertainty. Two processes are largely responsible for the GrIS contribution to SLR: (1) dynamic mass loss due to retreat and acceleration of outlet glaciers (40 %) and (2) increased surface melt induced by atmospheric warming (60 %) (Khan et al., 2014; Van Den Broeke et al., 2016). The first process which is most pronounced for marine terminating outlet glaciers (Moon et al., 2012), is potentially caused by an increase in submarine melting, which can in turn be attributed to a warming of the subpolar North Atlantic ocean, induced by circulation changes, and increased subglacial discharge (Straneo and Heimbach, 2013). ~~Regarding the latter mechanism, the maximum contribution due to~~ The maximum contribution of increased surface melt is estimated to range between 50 to 130 mm by the year 2100 (Fettweis et al., 2013). Due to the possibility of applying relatively high-resolution regional climate models, confidence in this estimate has increased in the recent years (van den Broeke et al., 2017). The contribution of the ~~second process~~ dynamic mass loss, however, remains highly uncertain because processes related to the response of marine terminated Greenland glaciers are still not properly represented in the contemporary GrIS models (Straneo and Heimbach, 2013; Khan et al., 2014; Goelzer et al., 2017).

The principal objective of this paper is to quantify the response of marine terminating outlet glaciers to future submarine melting and to analyze whether the impacts of ice-ocean interaction on SLR are comparable to long-term changes in surface mass balance (SMB).

In order to assess Greenland's contribution to future sea level rise, several different model strategies have been proposed. The most common method is to use three-dimensional ice sheet models, tuned to present-day conditions, and apply future climate change projections based on global or regional climate models. However, such models still have relatively coarse spatial resolution and cannot properly resolve most of the outlet glaciers that terminate in Greenland's fjords. Peano et al. (2017) investigated the 5 biggest ice streams and outlet glaciers in Greenland with a 3D ice-sheet model on a resolution of 5 km. Seddik et al. (2012) and Gillet-Chaulet et al. (2012) included improved model physics by using a full-Stokes approach and refined resolution over fast flow regions with adaptive mesh techniques. Their setup however, did not yet allow to simulate glacier retreat. Most of the ice-sheet simulations also do not describe the interaction between glaciers and the ocean explicitly, but in some cases, for instance in Fürst et al. (2015), ocean melting is parameterized indirectly by increasing the basal sliding factor as ocean temperature increases. For the RCP scenario 8.5, they calculated a SLR between 155 and 166 mm at the year 2100 for the entire ice sheet applying atmospheric and oceanic forcing. For regional settings, 3D models with a simple ocean melting parameterization were applied to study the historical (last 20 -30 years) retreat of Jakobshaven Isbrae (Muresan and Khan, 2016; Bondzio et al., 2017). A more advanced treatment of submarine melt rate was ~~done~~ used by Vallot et al. (2018).They coupled a plume model based on the Navier-Stokes equations with a full-Stokes ice sheet model. With this off-line coupling, glacier dynamics for one melt season were simulated for Kronebreen Glacier in Svalbard.

Another method, followed by Nick et al. (2013), is to simulate single outlet glaciers individually using a one-dimensional (1D) flowline model. Nick et al. (2013) performed simulations for four outlet glaciers that collectively drain about 22 % of the total solid ice discharge of the Greenland Ice Sheet. Assuming proportionality between the future contribution to SLR and present-day ice discharge, Nick et al. (2013) scaled up results obtained from four glaciers to the total estimate of all Greenland outlet glaciers, which resulted in a range between 65 and 183 mm by the year 2100. Taking this one step further, Goelzer et al. (2013) used the results from Nick et al. (2013) in a 3D coarse-resolution ice sheet model. They applied the 1D glacier thinning and grounding-line retreat scenarios as an external, pre-calculated forcing in the grid cells at the ice sheet boundary. Since only four glaciers had been simulated in the 1D model, they mapped the forcing from the original glaciers onto all other Greenland's marine terminating outlet glaciers with a nearest neighbour approach. The incorporation added only 8 to 18 mm SLR on top of the stand-alone 3D ice sheet model simulation. Goelzer et al. (2013) argued ~~, that the smaller contribution results from smaller marine terminating glacier that fully retreat~~ that the rather small contribution compared to Nick et al. (2013) is caused by the full retreat of the small marine terminating glaciers in the 3D ice simulations ~~, leaving no more~~within in a short timescale. When fully retreated, they do not experience any ice-ocean ~~, which is still included by the upscaling from Nick et al. (2013)~~ interaction any more. This loss of ice-ocean interaction, however, is neglected by the upscaling-method from Nick et al. (2013) and therefore leads to higher numbers of total SLR.

Since we are especially interested in the impacts of ice-ocean interactions on glacier dynamics and want to investigate numerous glaciers, we followed an approach similar to Nick et al. (2013) but for different glacier-types and with one notable improvement~~.: For~~ : for calculations of the vertically distributed submarine melt, we use a turbulent plume parameterization following Jenkins (2011). According to this parameterization, the submarine melt rate depends not only on ambient water temperature in fjords but also on seasonally varying subglacial discharge, shape and angle of the glacier tongue. The first idealized simulations of a coupled flowline-plume model were carried out by Amundson and Carroll (2018) by using the maximum melt rate as a frontal ablation factor to account for undercutting plus calving of tidewater glaciers, demonstrating the potential impact of the subglacial discharge on glacier dynamics. ~~For the evolution of the surface mass balance, we used anomalies computed by the regional climate model MAR and corrected them for surface elevation change~~While their study emphasizes the importance of subglacial discharge, their model setup does not allow for the evolution of floating tongues. Thus, we follow a different approach (section 2) to simulate the glacier profile more realistically.

We perform simulations for 12 representative Greenland glaciers (compared to four in Nick et al. (2013)). This enabled us to test the assumption used in Nick et al. (2013) that the contribution of individual Greenland outlet glaciers to SLR is proportional to their present-day discharge and therefore the total contribution of Greenland outlet glaciers can be obtained by scaling up contribution of individual glaciers proportionally to the entire present-day discharge of all outlet glaciers. In particular we derived a proportional factor between present-day grounding line discharge and future SLR using results of simulations for all twelve glaciers. We also estimated the uncertainties in the contribution of Greenland glaciers to SLR resulting from uncertainties in calving and ocean melt parameters and ~~climate change scenarios~~ocean warming.

The paper is structured as follows. First, we describe the coupled flowline-plume model, then how the input data were ~~preprocessed~~ pre-processed together with the experimental setting and climate change scenarios. Finally, we present the results of our model simulations for present day and future scenarios.

2 The coupled flowline-plume model

Most of Greenland's outlet glaciers terminate in fjords that are connected to the ocean. Inside these fjords, observations of upwelling plumes along the edges of glaciers have drawn attention to the potential importance of submarine melting. Consequently, considerable efforts in the modeling of submarine melt rate have been undertaken by using high-resolution 3D and 2D ocean general circulation models that are tuned to or parameterized after the buoyant-plume theory (Sciascia et al., 2013; Xu et al., 2013; Slater et al., 2015; Cowton et al., 2015; Carroll et al., 2015; Slater et al., 2017). However, such models are too computationally expensive and therefore impractical for simulating the response of the entire GrIS to climate change on centennial timescales. At the same time, recent studies demonstrate that the simple line plume model by Jenkins (2011) is an adequate tool to simulate plume behavior (Jackson et al., 2017) and to determine submarine melt rates for marine terminated glaciers (Beckmann et al., 2018). Since the plume model is significantly less computationally expensive than 3D ocean models, it represents an alternative approach to introduce ice-ocean interaction into the GrIS model and still maintain the model's ability to perform a large set of centennial-scale experiments. Simulating the glacier dynamics with 3D ice sheet models requires very high spatial resolution ($\ll$ 1 km) resulting in high computational cost (e. g. Aschwanden et al., 2016) and so far they cannot be used for centennial timescales. To reduce the computational cost we use instead a ~~1D~~ depth- and width- integrated one-dimensional ice flow model (Enderlin and Howat, 2013; Nick et al., 2013) coupled to a line plume model (Beckmann et al., 2018).

2.1 Glacier model

The governing equations of the 1D model include mass conservation:

$$\frac{\partial H}{\partial t} = -\frac{1}{W}\frac{\partial (UHW)}{\partial x} + \dot{B} - \dot{M}, \tag{1}$$

where H is ice thickness, t is time, U is the vertically averaged horizontal ice velocity, W is the width and x is the distance from the ice divide along the central flowline. ~~Where~~ $\dot{B}$ and $\dot{M}$ are the surface mass balance and the submarine melt rate of ~~one~~ the glacier.

The conservation of momentum involves a balance between longitudinal stress, basal shear stress and lateral stress on the one hand, and driving stress on the other:

$$2\frac{\partial}{\partial x}\left(H\nu\frac{\partial U}{\partial x}\right) - A_s\left[(H-\frac{\rho_w}{\rho_i}h_b)U\right]^q - \frac{2H}{W}\left(\frac{5U}{EAWW_s}\right)^{\frac{1}{3}} = \rho_i g H\frac{\partial h_s}{\partial x}, \tag{2}$$

where h_s denotes the ice surface height, h_b the depth of glacier below sea-level, ρ_i and ρ_w the ice and sea water density, respectively. The sliding law follows Nick et al. (2010) with the basal sliding coefficient A_s and the velocity exponent q, and the lateral stress involves a non-dimensional width-scaling parameter W_s. The lateral stress term likewise used by e.g. Nick et al. (2013); Enderlin and Howat (2013); Schoof et al. (2017), and originally derived by Van Der Veen and Whillans (1996), is necessary to account for lateral resistance in fast-flowing, laterally-confined glaciers typical for Greenland. Finally, the rate factor A and the enhancement factor E determine the viscosity ν

$$\nu = (EA)^{\frac{1}{3}}\left|\frac{\partial U}{\partial x}\right|^{-\frac{2}{3}}. \tag{3}$$

Calving occurs when surface crevasses propagate down to the water level (Nick et al., 2013). Crevasses depth d_s is calculated from the resistive stress $R_{xx} = 2\left(\frac{1}{A}\frac{\partial U}{\partial x}\right)^{1/3}$, as ice stretches, and can be enhanced by freshwater depth d_w:

$$d_s = \frac{R_{xx}}{\rho_i g} + d_w\frac{\rho_0}{\rho_i} \tag{4}$$

where ρ_0 is the freshwater density. The glacier front continuously advances over time, as the accumulated flux leaving the last grid cell is recorded and the calving front is advanced whenever the accumulated volume reaches the volume of a grid cell (assuming same thickness). Glacier front advance and calving are the two competing processes that determine the calving front position.

Initial boundary condition The boundary condition at the top of the glacier catchment is U(x=0) = 0, while at 0. At the calving front x_{cf} balancing , the balancing of the longitudinal stress with the hydrostatic sea water pressure and incorporating the incorporation of the flow law of ice yields longitudinal stretching

$$\left.\frac{\partial U}{\partial x}\right|_{x=x_{cf}} = EA\left[\frac{\rho_i g H}{4}\left(1-\frac{\rho_i}{\rho_w}\right)\right]^3. \tag{5}$$

The model employs a stretched horizontal grid with a horizontal resolution of 100 meters, where velocity is calculated at mid-points. At each time step of 3.65 days, the grid is stretched to keep track of the grounding line position, which is determined by the flotation floatation criterion

$$H_{\text{float}} \leq |z_b|\frac{\rho_{\text{w}}}{\rho_i}, \tag{6}$$

where z_b is the bedrock depth. Glacier thickness H and bedrock depth z_b of each cell interface are determined by linear interpolation between the cell centered values. Grid stretching is performed so that there is always a cell edge at the interpolated grounding line position. The new calving front position is determined so that the total glacier volume is not modified by interpolation. For every new point in the interior, model variables are interpolated from previous grid. The first grid point at the ice divide remains unchanged. If ~~ice grid~~ points on the new ice grid lie outside the ice domain ~~on the previous~~ of the previous ice grid, as it is typically the case for the last ice cell before the calving front, ice thickness from the last grid cell is extended to the new ice cell (the calving front advances).

The code is written is FORTRAN, following the numerical procedure of Enderlin et al. (2013). The main differences compared to their original matlab code[1] is that we include a subgrid-scale treatment of the calving front boundary, and an improved treatment of the submarine melting.

2.2 Plume model

The plume model equations account for a uniformly distributed subglacial discharge along the grounding line of a glacier , and contain the ~~the~~ evolution of the plume thickness D, velocity V, temperature T and salinity S along the direction of the plume.

$$q_s' = \dot{e} + \dot{m} \tag{7}$$

$$(q_s V)' = D\frac{\Delta\rho}{\rho_0} g \sin(\alpha) - C_d V^2 \tag{8}$$

$$(q_s T)' = \dot{e}T_a + \dot{m}T_b - C_d^{\frac{1}{2}} V \Gamma_T (T - T_b) \tag{9}$$

$$(q_s S)' = \dot{e}S_a + \dot{m}S_b - C_d^{\frac{1}{2}} V \Gamma_S (S - S_b) \tag{10}$$

The volume flux of the plume $q_s = DU$ (expressed per unit length in the lateral direction, i.e. $\mathrm{m^2 s^{-1}}$) ~~of the plume~~ is described by equation (7). It can increase by the entrainment of ambient seawater $\dot{e}$ and by melting $\dot{m}$ of ice from the glacier front. Equation (~~Eq.~~ 8) describes the balance between buoyancy flux and the drag $C_d U^2$ of the glacier front. The buoyancy flux is proportional to the relative density contrast $\frac{\Delta\rho}{\rho_0}$ between plume water and ambient water in the fjord (subscript a). This density contrast is ~~linear~~ linearly parameterized as $\beta_S(S_a - S) - \beta_T(T_a - T)$. The drag also results in a turbulent boundary layer (subscript b) at the ice-water interface, where melting occurs, and heat and salt is exchanged by (turbulent) conduction-diffusion. The temperature T and salinity S of the plume (Eq. 9,10) are determined by the entrainment of ambient water and the addition of meltwater, as well as by conduction fluxes at the ice-water interface (i.e. between boundary layer and plume). The entrainment rate is calculated as $\dot{e} = E_0 U \sin(\alpha)$, proportional to plume velocity and glacier slope, with the entrainment coefficient E_0.

The submarine melt rate along the path of the plume $\dot{m}$ is determined by solving the equations of heat and salt conservation at the ice-water interface:

$$\dot{m}L + \dot{m}c_i(T_b - T_i) = cC_d^{\frac{1}{2}} V \Gamma_T (T - T_b) \tag{11}$$

$$\dot{m}(S_b - S_i) = C_d^{\frac{1}{2}} V \Gamma_S (S - S_b) \tag{12}$$

[1]available at https://sites.google.com/site/ellynenderlin/research

where T_i and S_i, c_i are the temperature, salinity and the specific heat capacity of the ice and c the specific heat density for sea water. At the ice water interface the freezing temperature T_b is approximated as a linear function of depth Z ($Z < 0$) and salinity of the boundary layer S_b:

$$T_b = \lambda_1 S_b + \lambda_2 + \lambda_3 Z \tag{13}$$

with $Z = Z_0 + x \cdot \sin(\alpha)$, where Z_0 is the depth (negative) at the grounding line ($x = 0$). The algorithm for solving the set of equations and a list of all parameter values are provided in Beckmann et al. (2018).

The plume is a 1D model and therefore can neither simulate variability across the calving front (Fried et al., 2015), nor account for fjord wide circulation (Slater and Straneo, 2018) across and outside plumes. However, the width-averaged melt rates - as required for the 1d glacier model- can be simulated with the 1D plume model (Beckmann et al., 2018). We set the entrainment parameter E to 0.036, as suggested by Beckmann et al. (2018). Since the plume model in some cases underestimates and in others overestimates submarine melt rates (Beckmann et al., 2018), we also scale the simulated melt rate profile by a constant factor β, which we treat as an additional tuning parameter within the range 0.3 - 3 possibly different for each glacier (see section 4.1). The plume model employs a fine spatial resolution of about 1 m.

2.3 Coupling between glacier and plume model

Unlike Amundson and Carroll (2018), who used the maximum melt rate as a frontal ablation factor for tidewater glaciers, we take into account the entire profile along the submerged part of the outlet glacier to calculate the submarine melt rate with the plume model. Submarine melting volume flux is calculated for each cell and is applied as a vertical thinning rate on the floating tongue ($x_{g+1}...x_c$), or on the last grounded cell (x_g) in the case of tidewater glaciers (no floating tongue). The melt rate $\dot{m}$ is integrated from the grounding line (position x_{gl}) along the bottom face of the floating tongue (if any), and along the calving face (position x_{cf}) up to sea level (Fig. 1), or to the top height of the risen plume (which can stop below sea level). The total submarine melt rate over the glacier tongue (if any) for one outlet glacier is given by

$$M = \int \dot{m}(s)\, ds = \int\limits_{x_{gl}}^{x_{cf}} \dot{m}(h_b(x)) \cdot (\cos\alpha)^{-1} dx + \int\limits_{h_b(x_{cf})}^{0} \dot{m}(z) dz, \tag{14}$$

where s is the distance coordinate along the tongue bottom and the vertical calving face, h_b denotes bottom ice elevation, and $\cos\alpha$ is the variable tongue slope (calculated from the relation $\tan\alpha = \frac{\partial h_b}{\partial x}$). The integral is partitioned over various glacier cells (or only one cell (x_g) in the case of a tidewater glacier, where the first integral term is zero since $x_{gl} = x_{cf}$). This total submarine melt rate, in a cell by cell basis, is substituted in (the discrete form) of equation (1):

$$M_i = \int\limits_{x_{i-\frac{1}{2}}}^{x_{i+\frac{1}{2}}} \dot{m}(s)\, ds + \varepsilon_i \int\limits_{h_b(x_{cf})}^{0} \dot{m}(z) dz, \tag{15}$$

where ε_i is 1 if i represents the last ice cell ($x_i = x_c$), or 0 otherwise. The submarine melt rate $\dot{M}$ per units of length for each glacier cell (dx) in Eq. 1 is

$$\dot{M}_i = \frac{M_i}{dx} \tag{16}$$

~~.~~If there is no floating tongue, submarine melting is applied to the last grounded cell, otherwise it is applied starting from the first floating cell.

Thus the submarine melt rate reduces the thickness of the glacier cell. A reduced thickness at the first floating cell or last grounded cell leads to grounding line retreat since the grounding line position is determined by interpolation of the ice thickness above flotation at each time step. ~~Thinning the last floating cell leads to calving front retreat by either meltingthe total cell~~ Calving front retreat can be reached by melting/thinning the last floating ice cell completely or by calving, which increases with thinning.

Since the plume model does not allow for negative values of α, its minimum value is set to 10^{-6}. If the plume already ceases before reaching the calving front x_{cf}, we numerically introduce a minimal background melting determined by the last melt rate value before the plume ceased. At the calving front we calculate a 2nd plume that starts at $h_b(x_{cf})$ with the initial minimum default discharge value of $10^{-6}\ \mathrm{m}^3\ \mathrm{s}^{-1}$ to assure a background frontal melting.

Subglacial discharge Q for each glacier was computed off-line from the output of simulations with the ice sheet model SICOPOLIS (Calov et al., 2018) which includes explicit treatment of basal hydrology (Section 3.3). It is applied to the line plume (Fig. 2), assuming a uniform distribution of subglacial discharge along the width of the grounding line: $q_s = Q(W)^{-1}$. It is assumed that plume properties (velocity, temperature, salinity, and thickness) adapt instantaneously to changes in the glacier's shape, subglacial discharge, temperature and salinity profiles of ambient water. The glacier and plume model exchange information at every time step of the glacier model (Fig. 2).

3 Model Input

To simulate the response of the glacier-plume model to future global warming we considered the potential changes of surface mass balance (SMB) and submarine melting. To this end, for each glacier, we derived data sets for three forcing factors from the year 2000 till 2100: spatially distributed SMB (section 3.3), subglacial discharge (section 3.3) and fjord water temperatures (section 3.4). For changes in SMB we used anomalies from the simulation with the regional climate model MAR, forced by global GCM MIROC for the RCP8.5 scenario. In our previous study (Calov et al., 2018) we used the same SMB changes toforce the 3D ice-sheet model SICOPOLIS . Now we use results of this simulation to compute the subglacial discharge for each glacier from simulated surface runoff . Changes in ocean temperature were included by applying a linear warming trend, derived from several different CMIP5 models. On every time step the three forcing factors where provided as data-input and forced the glacier-plume model (Fig. 2).While for each glacier the future evolution of the subglacial discharge and ocean temperature where firmly prescribed in the data-sets, the SMB-input was interactively corrected for the surface elevation feedback and thus considered the glacier surface height on each time step. The upcoming subsections describe the choice of glaciers, how the geometry for the 1D model was derived and how the corresponding forcing factors were determined and applied.

3.1 The choice of glaciers

In this study ~~,~~ we modeled twelve ~~,~~ well-studied Greenland outlet glaciers of different sizes and located in different regions of Greenland (Fig. 3). One criterion for this selection ~~is~~ was that the glaciers should represent different types of ice flows and different environmental conditions. We also ~~include~~ included small marine terminating glaciers to assure a more realistic upscaling ~~Goelzer et al. (2013)~~(Goelzer et al., 2013). Besides that, for most of the chosen glaciers, Enderlin and Howat (2013) estimated submarine melting to calving ratios (grounding line mass flux lost by submarine melting divided by mass loss of calving) ~~which we use~~ were used as an additional constraint on the choice of modeling parameters.

3.2 Glacier geometry

For each individual glacier, bedrock elevation and width were determined by ~~analyzing~~ analysing cross-sections taken at regular intervals along the glacier flow, generally covering a large portion of the glacier catchment area (Perrette et al., in prep). In each cross-section, the procedure comes down to calculating a flux-weighted average for bedrock elevation, ice velocity U and thickness H, and ~~choose~~ choosing the glacier width W such that the flux F through the cross-section is conserved, i.e. $W = F/(UH)$. We ~~use~~ used the BedmACHInev2 data for bedrock topography (Morlighem et al., 2014). Fjord bathymetry was extended manually by considering available data (Mortensen et al., 2013; Schaffer et al., 2016; Dowdeswell et al., 2010; Syvitski et al., 1996; Rignot et al., 2016). For ice velocity we use data from Rignot and Mouginot (2012). The resulting glacier profiles are depicted in Fig. 6.

3.3 Subglacial discharge and glacier surface mass balance

To force the plume model, we ~~use~~ used monthly averaged subglacial discharge. Subglacial discharge represents the sum of basal melt (melt under the grounded ice sheet), water drainage from the temperate layer and surface runoff. The former two sources ~~are~~ were computed directly by the ice sheet model SICOPOLIS (Calov et al., 2018). In reality surface runoff can travel along the ice surface until it either reaches an existing connection to the bedrock (e.g. crack) or it accumulates in a supraglacial lake that eventually drains, making a new connection. However, these processes are ~~too~~ complex and still poorly understood. This is why in the relatively coarse (5 km) resolution ice sheet model (Calov et al., 2018), these small-scale processes ~~are~~ were neglected and it ~~is~~ was assumed that runoff penetrates directly down to the bedrock. The surface runoff and SMB anomalies for future scenarios are taken from experiments with the regional climate model MAR (Fettweis et al., 2013) and corrected for the future surface elevation change (Calov et al., 2018). The entire basal water flux (runoff, basal melt, and water from the temperate layer) ~~is~~ was routed by the hydraulic potential using a multi-flow direction flux routing algorithm, as described in ~~(Calov et al., 2018)~~Calov et al. (2018). All water transfer ~~is~~ was assumed to be instantaneous. Water that passes through the boundary of prescribed SICOPOLIS ice mask ~~is~~ was assigned to the closest glacier within a maximum distance of 50 km.

This maximum distance is necessary in areas where only few named glacier positions are available (mostly in the South of Greenland) and the distance between glaciers is large. For most of the coastline, especially in the area of our selected glaciers, this distance ~~has~~ had no effect on the results. We did not separately study the uncertainty in subglacial discharge related to this approach, but rather accounted for this uncertainty implicitly through the uncertainty of the scaling coefficient β for the submarine melt rate (see chapter 4.1).

In our future scenarios, when simulating subglacial discharge, we accounted for changes in surface runoff, basal melt, and ice sheet elevation~~but neglect the effect of ice sheet boundary retreat. This means that we route the subglacial discharge always~~. The routing end-points, that determine the amount of subglacial discharge for each glacier, however, were set constant to the present-day position of the ice sheet margin~~to determine the amount for the specific glacier. For neighboring~~. For neighbouring glaciers with a competing catchment area, a strong ice sheet retreat may strongly affect the distribution of the subglacial discharge between those glaciers (Lindbäck et al., 2015). This effect ~~is~~ was not included in this study.

In this study, we ~~use~~ used a single scenario for future surface runoff and SMB change, namely, a simulation with the regional model MAR nested in the global GCM MIROC5 model forced by the RCP 8.5 scenario. Among the CMIP5 models, MIROC5 ~~simulate~~ simulates climate change which ~~leads~~ led to a medium contribution of GrIS to future SLR (Calov et al., 2018). To correct for global climate model biases in surface runoff and SMB, we used anomalous approach by adding future anomalies in surface runoff and SMB simulated by MAR nested into the MIROC5 model to the reference climatology (reference period 1961-1990) simulated by MAR forced by ERA reanalysis data. We also corrected model surface runoff and SMB for changes in surface elevation by applying the gradient method of Helsen et al. (2012) as described in Calov et al. (2018). The surface runoff R over the ice sheet (SICOPOLIS) is determined as

$$R(x,y,t_{monthly}) = R^{\mathrm{Clim\ 1961-1990}}_{\mathrm{MAR(REAN)}}(x,y) \quad + \quad (R_{\mathrm{MAR(MIROC)}}(x,y,t_{monthly}) - R^{\mathrm{Clim\ 1961-1990}}_{\mathrm{MAR(MIROC)}}(x,y)) \\ + \quad \left(\frac{\partial R}{\partial z}\right)_{\mathrm{MAR(MIROC)}}(x,y,t) \quad \Delta h_s(x,y,t_{monthly}), \tag{17}$$

where the runoff $R(x,y,t)$ on every grid cell (x,y) at any time t ~~is~~ on a monthly time-step was calculated by the climatological mean from 1961-1990 of MAR (forced by reanalysis data) $R^{\mathrm{Clim\ 1961-1990}}_{\mathrm{MAR(rean)}}(x,y)$ plus the anomaly of the runoff relative to the climatological mean for the same period of time obtained by MAR forced with MIROC5 $(R_{\mathrm{MAR(CMIP5)}}(x,y,t) - R^{\mathrm{Clim\ 1961-1990}}_{\mathrm{MAR(CMIP5)}}(x,y))$. For ice surface evolving in time $\Delta h_s(x,y,t) = h_s^{\mathrm{obs}}(x,y) - h_s(x,y,t)$, the vertical gradient $\left(\frac{\partial R}{\partial z}\right)_{\mathrm{MAR(MIROC)}}(x,$ determined for every time step, ~~is~~ was additionally applied to ~~accounting~~ account for the increase in surface runoff. The observed surface elevation h_s^{obs} of the ice sheet ~~is~~ was taken from Bamber et al. (2013). Negative runoff values ~~are~~ were set to zero. The correction of runoff for elevation change can be important in some case since, as it was shown in Amundson and Carroll (2018) ~~,~~for tidewater glaciers, large and rapid changes in glacier volume can lead to a high increase in runoff due to surface lowering.

For the present-day condition, ~~SMB is~~ the SMB for the glaciers was calculated from relaxation to observed surface elevation h_s^{obs}, with a different relaxation time scale τ for each glacier (see section 4.1):

$$\dot{B} = \frac{h_s^{\mathrm{obs}} - h_s}{\tau} \ \text{in m/yr.} \tag{18}$$

With the latter equation we ~~calculate~~ calculated the present-day SMB during the spinup experiment, similarily to Calov et al. (2018). For future scenarios, we added the anomaly of the SMB (relative to the year 2000) to the present-day SMB. The anomaly for each grid cell of the glacier was computed from interpolation of the MAR anomaly of the centerline of the individual glacier and additionally corrected for the glacier elevation change similarly to the surface runoff (Eq. 17), but for the SMB-calculation, Δh_s is the glacier elevation change compared to present-day, assuming that the derived glacier shape from the present-day dataset is for the year 2000. The time series of cumulative SMB (without surface correction) and the annual subglacial discharge for each glacier are shown in the supporting information (Fig. S1 and Fig. ~~S4~~S2)

3.4 Fjord temperature and salinity profiles: CTD measurement and Ocean Reanalysis data

Determining vertical temperature and salinity profiles in Greenland fjords, which are the input for the plume model, is a challenging task. Measurements inside Greenland fjords are rare and do not cover all of them. For some fjords, several conductivity-temperature-depth (CTD) measurements exist, but they are mostly infrequent and often not performed close enough to the calving front. It is also important to note that T-S profiles obtained from CTD measurements have to be treated with caution because they represent only a 'time shot' of fjord properties which vary ~~in time significantly (Jackson et al., 2014).~~ significantly in time (Jackson et al., 2014).

However, the question arises on how to treat fjords, where no CTD measurements are available. A possible solution is to use ocean reanalysis data. Here we use the TOPAZ Arctic Ocean Reanalysis data[2] (Xie et al., 2017) and compare them with existing CTD measurements. Note that for all twelve glaciers used in this study the CTD measurements from the adjacent fjord are available and we use them throughout our experiments as the preferred Temperature-Salinity-profile (TS-profile). ~~Nevertheless, to~~ To make assumptions on potential impacts of the differences between reanalysis and CTD profiles on the glacier response to climate change we investigate both types of ocean data (reanalysis and measurements). ~~The TOPAZ dataset was produced with the ocean model HYCOM using in situ measurements and satellite data sets. It covers the time span from 1991–2013 with a spatial resolution of 12.5 km and for depths of 5, 30, 50, 100, 200, 400, 700, 1000 … 3000 m. Below 200 m depth an error $> 1°$C and > 0.1 psu can occur. The dataset does not resolve the Greenland fjords and covers only the open ocean and continental shelf.It is known that the vertical T-S profile inside the fjords can resemble the profile in the open sea (Straneo et al., 2012; Straneo and Heimbach, 2013; Inall et al., 2014). However, often the closest grid cell in the ocean reanalysis data which corresponds to the depth of the grounding line can be located hundreds of km from the fjord mouth, where other ocean conditions might prevail. Figure **??** illustrates this problem for the Kangerlussuaq glacier: CTD measurements below 400 m show here much colder temperatures inside of the fjord than far outside of the fjord. A calculation~~

[2] http://marine.copernicus.eu/services-portfolio/access-to-products/?option=com_csw&view=details&product_id=ARCTIC_REANALYSIS_PHYS_002_003

with the line plume for a subglacial discharge of $50\ \mathrm{m^3\,s^{-1}}$shows that the melt rate calculated with the TS-profile inside the fjords (50 km away from glacier) and on the continental shelf (200 km away from calving front) gives similar values of $0.5-0.6\ \mathrm{m\,d^{-1}}$ but when the melt rate is calculated using the outermost CTD outside the continental shelf (Fig. **??** red dot, at $\sim$ 400 km distance from the glacier and where the nearest reanalysis data with the 700 m depth are available) simulated melt reaches $3.6\ \mathrm{m\,d^{-1}}$, i.e. nearly an order of magnitude higher. Thus, choosing temperatures in the open ocean may lead to strong errors of simulated melt rates. Due to all these uncertainties, here we test how sensitive the model response is to the chosen present-day T-S profile (CTD or Reanalysis) when carrying out future climate change simulations (Section 5).To this aim, we first compared temperature-salinity profiles constructed from Figure 4 illustrates the strong bias towards colder temperatures for the reanalysis data to available CTD measurements inside the fjords made near to the glacier fronts. We investigated how to use the reanalysis data from outside the fjords to produce T-S profiles close to observations made inside the fjord. We firstly constructed the T-S profiles from reanalysis data by detecting the reanalysis grid-cells closest to the fjord mouth and with the depth of at least 200, 400 and 700 meters. We chose these maximum depths, since they corresponds vertical levels in set. The detailed description on how the temperature profiles were derived from the reanalysis data set and at the same time represent typical depths of Greenland fjords and glacier grounding lines. Surface temperatures can be strongly influenced by a seasonal signal or other external factors and since they are less important for determine the submarine melt rate, we asses the quality of the constructed T-S profile by comparing with CTDs temperatures at the depths 200, 400 and 700m only. Figure **??** and **??** compare the temperature at these depths from reanalysis data with available CTD profiles measured over past several decades for Jakobshavn-Isbrae and Store Glacier. Since Greenland is surrounded by the continental shelf with typical depths of 200–400 meters, most of the 700-meter depth grid-cells in the reanalysis data are located outside the shelves, far away from the glacier mouth as shown in Fig. **??** on the example of Store Glacier. For Store Glacier, the temperature at 700m depth inside the fjord measured by CTD is much warmer than the temperature in reanalysis data at the same depth but far away in the open ocean, which can potentially be explained by the influence of shallow continental shelf. As Schaffer et al. (2017) showed, for the Nioghalvfjerdsfjorden Glacier, the continental shelf works similarly to a sill that blocks waters from greater depths and favors shallow water masses to pass into the fjord. For all of the investigated glaciers, we found better agreement between temperature profiles constructed from the reanalysis data and CTD if we disregard temperature at 700m-depth in reanalysis data and use instead temperature at 400m-depth only mainly located on the continental shelf. If the grounding line depth was deeper than 400 m, temperatures below this depth were assumed to be equal to the temperature at 400m-depth in the reanalysis data. The corresponding salinity profile below 400m-depth was modified the same way as the temperature profile. The location of the reanalysis data point is listed in Table 1 of the illustrations of both temperatures profiles that forced the glacier-plum model can be found in the supporting information. To produce a "present-day" reanalysis T-S profile that resembles inside-fjord conditions, we averaged temperature and salinity from reanalysis data over period 1990–2010 in that particular cell. An overview of the the T-S profiles from CTD and constructed from reanalysisdata is given in the supporting information (Fig. S3) .

The T-S profiles constructed from the reanalysis data, as well as those from the CTD measurements, were used as the boundary conditions for the plume model. Figure 4 shows that the temperatures derived from reanalysis data are colder than those from CTD measurements at the grounding line depth for most of the selected glaciers. This bias also remains when choosing temperatures from reanalysis data for the same periods when the CTD measurements were taken (not shown). Similar to the continental shelf, 'blocking' shallow sills in a fjords modify the water masses near the grounding line of a glacier. However, considering of the sill depth (Fig. S2, supporting information) when reconstructing the T-S profiles from the reanalysis data only leads to an even stronger temperature bias (dashed line Fig. S3, supporting information). Therefore, we always use the reanalysis data from 400m depth to construct T-S profiles irrespectively of the sill's depth. In the following section, we investigate how the discrepancy of T-S profiles from CTD and reanalysis data may affect glacier response to future climate change.

Thus, for each glacier, we have two temperature profiles (CTD and reanalysis) that are used to simulate the present-day submarine melt rate in the spin-up experiment. We did not consider a seasonal cycle since this would only be represented in the upper surface layer, which of less importance for the calculation of the submarine melt rate. For future simulations, we prescribed simple scenarios for the ocean temperature anomalies based on (ΔT) based on minimal and maximal temperature trends simulated by several CMIP5 models (GFDL-ESM2G, MPI-ESM-LR, and HadGEM2-CC). The trend is added to the T-S uniformly to the entire Temperature profiles (both CTD and reanalysis) for the future simulations.

$$T(Z,t) = T(Z)_{\mathrm{CTD/REAN}} \pm \Delta T_{\mathrm{min/max}} \cdot t \tag{19}$$

To determine this temperature trend we use the closest to the fjord model grid-cell with the ΔT for each CMIP5 model we used the grid-cell closest to each fjord but with a depth larger than 400mfor each CMIP5 model. The temperature trends were approximated by linear regression as illustrated in Fig. 5. The Figure shows as well, also the big discrepancy between the model temperatures and CTD measurement at 700m depth which was the motivation to use 400 m depth only. The temperature trends and cell locations for each glacier and CMIP5 model are listed in Table S1 of the supporting information, while the resulting minimal and maximal temperature trends of these trends for each glacier $\Delta T_{\mathrm{min/max}}$ are listed in Table 1.

4 Experimental setup

4.1 Selection of model parameters and model spin up

Model calibration and spinup for each glaciers have glacier has been made in two steps. First, the stand alone glacier model (without the plume parameterization) was pre-calibrated to best match observed surface elevation, grounding-line position (accuracy $\pm 2\,\mathrm{km}$ has been required) and velocity profile assuming a constant prescribed submarine melt rate. Dynamic parameters E, W_s, A_s and q (equation 2) were varied for this purpose (affecting basal shear stress, lateral stress, and calving front boundary condition), along with the freshwater depth in crevasses d_w and the constant melt rate m, for each glacier separately. The values of dynamic parameters and relaxation time scales for each glacier are listed in the supporting information table Table S2.

Once the four dynamic parameters and the relaxation time scale are set in our pre-calibration, we performed a set of spin-up experiment with the coupled glacier-plume model for each glacier. In the spin-up experiments the submarine melt rate is now simulated interactively by the plume model which requires subglacial discharge and temperature and salinity profiles as input-data. We used monthly subglacial discharge for the year ~~2000.~~ 2000 derived from SICOPOLIS (section 3.3). Vertical temperature and salinity profiles in these experiments were taken from the reanalysis data, averaged over the time interval 1990–2010 or from recent CTD data, and were held constant in time (Fig. S3, supporting information). Nonetheless, in the spin-up experiments the submarine melt rate is not constant since changes in the grounding line depth and shape of ~~a~~ the floating tongue (if ~~exist~~present) affect the submarine melt. We chose the year 2000 as the quasi-equilibrium initial state for "future" climate change simulations since the mass loss of GrIS during the last decade of ~~20the~~ the 20th century was rather small (ca. 0.1 mm/yr in sea level equivalent) ~~compare to that has been~~ compared to that observed in the first decade of the 21st century ((Vaughan et al., 2013).

We generate an ensemble of model realizations by varying two model parameters: freshwater depth in crevasses d_w and the plume linear scaling parameter β, (factor in a range from 0.3 to 3 that multiplies the simulated melt rate profile), which control calving rate and submarine melting, respectively. We run the coupled model for each combination of these two parameters over 100 years, so that the glacier at the end of the simulation was close to an equilibrium state and we exclude model versions which simulated the grounding line position ~~with the error~~ more than 2 km distant from the observed one or which displays a low-frequency oscillatory behaviour with advancing glacier front over the last 20 years of simulations. The list of the parameter range and number of valid realizations for CTD and reanalysis data can be found in the supporting information, Tab. S3. For the glaciers for which partition between calving and submarine melting was available from Enderlin and Howat (2013), we used this partition as an additional constraint for the model parameter combinations.

4.2 Future climate scenarios

For all future simulations, we used valid combinations of model parameters and corresponding initial conditions obtained at the end of the 100-yrs spin-up runs. The anomalies of SMB were derived from the regional climate model MAR simulations as described in Section 3.3 (Fig. S1, supporting information). To compute ~~the submarine melt rate~~future ocean temperature, we use the minimal and maximal ocean temperature trends (Table 1) added on the temperature-depth profiles for each glacier ~~listed in Table 1~~ (Section 3.4). We prescribe the subglacial discharge for each glacier ~~simulated~~ off-line with a monthly time step from the output of the ice sheet model SICOPOLIS. The yearly subglacial meltwater discharge is depicted in Fig. ~~S4~~S2. Figure 2 illustrates the data input required for each glacier to simulate their response to future atmospheric and oceanic warming.

All forcing scenarios were applied for the years 2000–2100. In addition, we run the model for 100 years with zero anomalies of temperature, SMB, and subglacial discharge to determine unforced model drift.

To express ice volume loss in sea level rise equivalent we used the multiplication factor ~~t~~ l under the assumption of oceans occupying $A_{\mathrm{ocean}} = 360 \cdot 10^6\ \mathrm{km}^2$:

$$tl = \frac{\rho_{\mathrm{ice}}}{\rho_{\mathrm{fw}} A_{\mathrm{ocean}}} \qquad (20)$$

leads to a SLR of $2.55 \cdot 10^{-3}$ mm for $1\,\mathrm{km}^3$ of ice volume V_{SLR} with the density of ice $\rho_{\mathrm{ice}} = 917\,\mathrm{kg\,m^{-3}}$, and fresh water $\rho_{\mathrm{fw}} = 1000\,\mathrm{kg\,m^{-3}}$.

The contributing ice volume V_{SLR} is determined by the lost ice volume above flotation from each glacier.

5 Results

5.1 Present-day state

The simulated present-day glacier thickness and velocity profiles for the different submarine melting and calving ratios are depicted in Fig. 6 with a close-up to the grounding line in Fig. S5, supporting information. Note that we allow for small floating termini, since many tidewater glaciers still evolve them on a seasonal scale and glacier fronts are also mostly undercut and thus missing a pure vertical cliff withouth any floating terminus (Bevan et al., 2012; Straneo et al., 2016; Rignot et al., 2015). Each lines line in the figure corresponds to a different combination of model parameters β and d_w listed in Tab. S3, supporting information. We found that for some glaciers, the grounding line demonstrates a high sensitivity to the melting/calving ratio, while others are primarily controlled by their bedrock topography and have relatively small variations in their grounding line position over the whole melting/calving ratio range. The Gade and Upernavik North glaciers are Upernavik Glacier is an examples of the latter case (Fig. S6S9 and S10, supporting information). In general, we observed higher velocities at the glacier terminus when higher calving rates were applied. Thus, if a glacier is not strongly buttressed by a sill or lateral resistance, different values of velocity at the glacier terminus due to different d_w strongly affect the equilibrium grounding line position. Such behavior points on the crucial role of the bedrock topography for glacier dynamics. The simulated realistic velocity profiles (Fig. 6) for Gade Glacier and Jakobshavn-Isbrae lead to a slightly thinner than observed glaciers. For Jakobshavn-Isbrae we were only able to achieve stable states using T-S profiles from the reanalysis dataset, since CTD measurements showed significantly warmer temperatures and the resulting high submarine melt rate lead led to the retreat of the glacier on the retrograde (upstream deepening) bedrock.

Table 2 provides a comparison of simulations with observational data derived by Enderlin and Howat (2013). Only the glaciers Kong-Oscar and Docker-Smith showed a grounding line flux $\mathrm{Flx_{gl}}$ matching the observational data. All other glaciers have smaller grounding line fluxes than in Enderlin and Howat (2013). However, it should be noted that many glaciers accelerated since 2000, so it is not clear whether the fluxes reported by Enderlin and Howat (2013) are directly comparable with our equilibrium fluxes. Additionally, Enderlin and Howat (2013) derived submarine melt rates for the floating termini of the glaciers only since they could not account for melting of vertical glacier fronts due to limitations of their methodological approach. For a direct comparison to Enderlin and Howat (2013), we calculate $\mathrm{MeltFlx}$ of the simulated glaciers by only considering the mass loss from the floating tongue induced by submarine melting. The ratios of submarine melting to grounding line discharge of our simulations lie within the uncertainty ranges determined by Enderlin and Howat (2013). However, these uncertainties are quite large and thus allow broad parameter combinations range for some glaciers. For Jakobshavn, a high calving flux was needed in order for the coupled glacier-plume model to obtain realistic present-day velocity profile for the coupled glacier-plume model (Fig. 6) . This results in simulated glacier profiles without any floating terminus ($\mathrm{MeltFlx} = 0$), which is not consistent with Enderlin and Howat (2013). Therefore, this simulated glacier does not match the ratio of submarine melting to grounding line discharge ratio given in Enderlin and Howat (2013) ($\mathrm{MeltFlx}^{\star\mathrm{E}}/\mathrm{Flx}^{\star\mathrm{E}}_{\mathrm{gl}}$ Table 2). The high calving flux required to obtain the precise grounding line position might result from an error in bedrock data or a problem with the flux-weighted averaging. The ~~Simulated~~ simulated Daugaard-Jensen Glacier only has a stable position with submarine melt rates lower than in Enderlin and Howat (2013).

5.2 Future simulations

After obtaining the present-day state (year 2000), we then ran the model ensemble with all valid combinations of the parameters β and d_w for 100 simulation years, applying MAR SMB anomalies, monthly subglacial discharge and two scenarios for ocean temperature change (minimum and maximum) as forcing. All results shown here have a small model drift subtracted from the calculated values, to ensure that the simulated SLR is a response to the climate change signal. The glaciers' response to climate change strongly depends on the combination of model parameters and scenarios, resulting in high uncertainty ranges. The simulations that led to a median-range[3] SLR for each glacier is depicted in Figure 7. After 100 years, some glaciers retreat entirely and become land-terminated (Alison, Daugaard-Jensen, Kangerlussuaq, Store), while others barely show a change in the position of the grounding line (Helheim). The individual contribution of each glacier to SLR for the median-range[3] SLR experiments is shown in Fig. 8 a. Jakobshavn-Isbrae shows the most significant contribution to SLR, due to the big catchment area and large retreat, followed by Kangerlussuaq Glacier due to its full retreat.

When forced by comprehensive climate change scenarios (changes in SMB with the surface elevation feedback, ocean temperature ~~T~~ T and subglacial discharge ~~Q~~Q) the median estimate for SLR contribution from all 12 glaciers is about ~~17 mm~~ 18 mm (17.9 mm) at the year ~~2100.~~ 2100 (Fig. 8 a, and Fig. 8 b, blue curve). To quantify the role of the individual forcing factors, we ~~perform~~ performed an additional set of ~~simulation with the~~ simulations with the same model versions corresponding to the median SLR response ~~by applying~~ (18mm) but applying the three different forcing factors ~~separately. We found that from the 17 mm over 70 % of SLR is caused by increased submarine melting due to the ocean warming T and increased subglacial discharge Q (Fig. 8 b). We found that both factors, T and Q, contributed an approximately equally to SLR. The reaming 30 % are attributed to the glacier's response to changes in SMB (~~in sequence. With the same model version we rerun for each glacier the experiment omitting changes in subglacial discharge (denoted "SMB + T" in Fig. 8 b, ~~orange curve). This is quite substantial, considering the fact that the SMB-forcing alone derived from MAR (without the glacier's response) has an almost negligible effect on SLR (~~pink curve) and omitting changes in subglacial discharge and ocean temperatures (denoted "SMB" in Fig. 8 b, ~~brown curve)~~sum of the brown, orange and yellow areas). The total effect of SMB change on SLR is decomposed into "static" (brown), "dynamic" (yellow) and effect of elevation correction (orange). "Static" effect was computed as the cumulative integral of SMB anomalies over the fixed present-day catchment and elevation of individual glaciers. As Fig. 8 b shows, this component is close to zero which is explained by the geometry of the glaciers' catchment area, where the ablation area is much smaller than accumulation area. For some glaciers, the cumulative SMB over the glacier~~'s catchment area even increases~~ 's catchment even increased towards the end of 21 century due to increased precipitation over accumulation area (Fig

[3]median for an odd number of simulations, the first value of higher half for an even number of simulation

S1, supporting information). ~~Whether this, anyhow minor SMB forcing (brown curve) is corrected for~~ Thus most of SLR due to SMB change alone occur through the dynamical processes – thinning and acceleration of glaciers, which in turn affects the calving rate. The surface elevation feedback (~~see Section 3.3)or not , is of no significance for SLR~~ Fig. 8 b, yellow curve). has only a minor effect on the glaciers response to SMB change which is not the case for the entire GrIS (Calov et al., 2018) where this effect is important. As explained above, we attribute 30 % of the 18mm SLR to the response to changes in SMB alone. The remaining 70 % of SLR is thus caused by the response to ocean warming and increased subglacial discharge (Fig. 8 b, ~~orange and yellow curve). The increased mass loss by glacier dynamics origins if surface mass loss is concentrated at the glacier terminus, resulting in thinning and potentially triggering glacier retreat.~~

~~These estimates of the role of separate factors (changes in SMB, ocean temperature and subglacial discharge)~~ blue and pink area together). We found that both factors, ocean warming and increased subglacial discharge, are of comparable importance for SLR (by comparing the blue and pink curve in Fig. 8 b These estimates are valid only for the cumulative SLR of all 12 glaciers. Each individual glacier may respond differently to the individual forcing factors. For instance, ~~the~~ Kong-Oscar Glacier (Fig.~~9~~ 9)) is slightly gaining mass with the SMB forcing alone and shows a retreat by 10 km and contribution 1 mm to SLR ~~only~~ due to ocean warming. When the increase in subglacial discharge is ~~considered additionally~~ added to the ocean warming, the glacier retreats another 10 km and contributes ~~approximately 3~~ additionally 2 mm to SLR.

At the same time, the Yngvar-Nielson Glacier (Fig. ~~9~~10) is already retreating significantly in the experiment with the SMB forcing alone. Ocean warming and increased subglacial discharge also contribute to SLR, but for Yngvar-Nielson the largest SLR contributor is the SMB change. The different dynamic responses of glaciers can be clearly seen for Rink-Isbrae Glacier and Store Glacier: Both have approximately the same SMB forcing (Fig. S1) but the unstable position of Store Glacier (on the tip of a steep sill, Fig. fig:tuning) causes the glacier to be more vulnerable to mass changes at the glacier terminus and when pushed to the retrograde bed the glacier automatically retreats and thus contributes to additional SLR. The dynamic response leads to a significant higher SLR for Store Glacier than for Rink Glacier.

Above we discussed only median-range scenarios, but the uncertainty ranges are crucial when projecting future SLR. Therefore, Fig. 11 shows the first and third quartile together with the median values of the individual glacier's contributions to SLR for all sets of valid model ~~realizations~~ realisations and full forcing (SMB + T (max/min) + Q) against the simulated present-day glacier discharge. Their potential SLR and grounding line retreat are listed in Table 3 and 4. Figure 11 shows a correlation between present-day grounding line discharge and the contribution to future SLR for individual glaciers. Jakobshaven and Kong-Oscar show the largest spread. ~~To analyze~~

The only 'uncertainty' in the ocean forcing is contained in the choice of the ocean temperature trend ($T_{\min}$ or $T_{\max}$). Thus, to analyse whether the uncertainty ranges in SLR result primarily from the ~~range of temperature~~ uncertainty range in the forcing or from the uncertainties ~~in model parameters~~of the model parameters/ the melting-to-calving proportion (uncertainty ranges in β and d_w) we show in Fig. 12 results of experiments forced only by $T_{\min}$ or $T_{\max}$ ocean warming scenarios. Figure 12 shows that future SLR and its uncertainty related to the glacier response to SMB forcing alone are rather small (except for Jakobshaven-Isbrae). ~~For glaciers like Rink and~~ Since the SMB forcing is the same in all simulations, the spread originates from the differences in initial states cause by different d_w and β combinations, thus different melting-to-calving proportion.

For Kong-Oscar Glacier, the negative SLR originates from the increase in SMB in this region under the RCP 8.5 scenario . Since there is only one SMB forcing the spread originates from the differences in initial states cause by different fwd and β combinations(Fig. S1). Including the forcing factors of submarine melt, T and Q, leads to a relatively high SLR contribution and high SLR uncertainty ranges for the Kong-Oscar, Kangerlussuaq, Rink, and Daugaard-Jensen glaciers, glacier (Fig. 12 shown by the blue columns). Since these high uncertainties arise also with the same forcing (only $T_{\min}$ or $T_{\max}$), we attribute the major source of uncertainty to the different combinations of the model parameters d_w and β. For each experiment, we also investigated whether the choice of using CTD measurements or reanalysis data for the initial ocean temperature profile had an impact on the potential SLR (Fig. S8S11, supporting information). If we neglect Jakobshaven and Kong Oscar glacier (almost no valid simulations with CTD profiles available), only Helheim glacier showed a stronger increase in SLR when reanalysis data where used to construct T-S profiles. For the rest of the glaciers the choice of using reanalysis data or CTD data for T-S profiles shows only minor differences in SLR. In

To approximate the total contribution of SLR of all glaciers we aim to upscale the results derived by the representative 12 glaciers, studied here. Thus, in spite of these uncertainties, we use the median scenarios from Fig. 11 to estimate the relationship between present-day glacial discharge and contribution to SLR for the year 2100 by fitting a linear regression determined with the least square method. The derived slope ($0.11\ \mathrm{mm\ km^{-3}\ a}$$0.12\ \mathrm{mm\ km^{-3}\ a}$) is statistically significant (p-values $=0$$< 0.01$) and has a correlation coefficient of 0.750.74. With this slope and the total flux of all outlet glaciers ($\sim 450\ \mathrm{Gt/a}$ (Enderlin et al., 2014; Rignot et al., 2008)), the simple linear relationship would imply a total SLR contribution of roughly 5 cm (53 54 mm) from all Greenland outlet glaciers at the year 2100. This upscaling method is very sensitive to the choice and amount of glaciers as Fig. 13 shows. When choosing only four glaciers (as in Nick et al. (2013)) to determine the slope of the regression line, the slope can range between $0.03 - 0.16\ \mathrm{mm\ km^{-3}\ a}$ (depending strongly on the choice of glaciers by picking the four glaciers that led to the most extreme cases, Fig.S7 supporting information)leading 13). This leads to an uncertainty range of roughly 15–80 mm, closely to Nick et al. (2013). These resulting regression line is overlapping with the higher uncertainty range of Nick et al. (2013)(65-183mm). Due to the low sample size of four glaciers, these resulting regression lines are however not statistically significant. This Nonetheless, the experiment underlines the importance of choosing a sufficiently large sample size and representative types of glaciers.

6 Discussion and Conclusions

For 12 selected outlet glaciers of the GrIS, we investigated their potential contribution to SLR during the 21st century for the RCP 8.5 scenario. To study the role of future changes in SMB, ocean temperature and subglacial discharge, we used a 1D flowline model which includes a surface crevasse calving law and is coupled to a the 1D line plume model of Jenkins (2011). In our model, the calving flux can be altered by choosing a parameter for the freshwater depth in crevasses, and the submarine melt rate can be changed by a scaling factor. We also used two different initial temperature-salinity profiles – one derived from reanalysis data and another from in-situ measurements inside the fjords. For the present-day simulations, we varied the submarine melting and the calving parameter to obtain a glacier profile similar to observations. For all outlet glaciers, we were able to achieve a reasonable agreement between the simulated and observed present-day profiles. However, for the Jakobshavn Isbrae glacier, the simulated submarine melt and grounding line discharge ratio does not agree with that derived by Enderlin and Howat (2013), as this ice stream could not develop a floating terminus in our simulations. The melt ratio derived by Enderlin and Howat (2013) could also not be achieved for Daugaard-Jensen.

In order to simulate the future glacial contribution to SLR under the RCP 8.5 scenario, we prescribed changes in SMB and subglacial discharge based on results of the regional climate model MAR. Anomalies of ocean temperatures from CMIP5 climate models were used to generate minimum and maximum scenarios for the ocean temperature change until year 2100. Simulated SLR contributions for the year 2100 compare well to values from Nick et al. (2013) for Jakobshavn Isbrae. The conservative estimations of Jakobshavn Isbrae contribution to SLR obtained with the 3D model of Bondzio et al. (2017) also lie within our uncertainty range. For ~~the~~ Kangerlussuaq Glacier our estimates ~~for~~ on SLR contribution exceed ~~estimation~~ the estimations of Nick et al. by 2 mm, while for ~~the~~ Helheim Glacier our SLR estimations are below the ~~estimation~~ estimations of Nick et al. (2013). In our simulations all glaciers experience a grounding line retreat which is found as well by Nick et al. (2013) but was not simulated by Peano et al. (2017). This discrepancy might be related to the coarse spatial resolution (5 km) of Peano et al. (2017) model (especially for the deep and narrow trough in Jakbobshavn) or processes upstream of the glacier might have counterbalanced the glacier retreat, which we could not simulate with a 1D flowline model. The difference to Nick et al. (2013) can be explained by their different treatment of calving processes (in their model freshwater depth in the crevasses was linked to runoff) or submarine melting (~~Nick et al~~ Nick et al. (2013) did not account on the influence of changing subglacial discharge). Also, Nick et al. (2013) used the surface elevation and velocity profile from the center line~~and~~. For Helheim glacier and Kangerlussuaq glacier they took the width of the whole catchment area ~~,~~ whereas at Jakobshaven Isbrae ~~,~~ the width was constrained to the width of the trough and ~~the~~ a constant lateral flux was added to gain the high grounding line flux of Jakobshaven Isbrae. By contrast, we ~~use~~ used a flux-weighted average of the whole glacier catchment area to represent each individual glacier.

We also investigated how different forcing factors influence the simulated future SLR. For the ensemble of the 12 glaciers, SLR ~~is over~~ was over a threefold larger when the changes in subglacial discharge and ocean temperature were added to changes in SMB. This underlines the critical role of ~~oceanic warming~~ submarine melting for future GrIS contribution to SLR. Moreover, we found significantly larger SLR when the subglacial discharge is allowed to increase in the scenarios. In fact, the amount of SLR attributed to subglacial discharge is similar to the SLR attributed to an increased ocean temperature. Thus, for future projections, both factors affecting submarine melt rate – subglacial discharge and ocean temperature – need to be taken into account. Also we show that even the almost negligible (compared to SLR) SMB-forcing results in a considerable contribution to SLR due to the dynamical response of the glaciers. This response, however is strongly controlled by the underlying bed topography of each individual glacier (e.g. Rink-Isbrae and Store Glacier). It should also be noted that our 1D flowline model is based on a crevasse depth calving law and thus does not account for undercut calving or buoyancy-driven calving (Benn et al., 2017), which in turn is strongly influenced by submarine melting. This mechanism might act as a further amplifier of glacial mass loss that is not accounted for in our results.

Our experiments also reveal large uncertainty ranges, primarily attributed to the different combinations of the two model parameters that determine submarine melting and calving fluxes. Nonetheless, the simulated melt/calving ratios lie within the uncertainty range of observations, and reducing the uncertainties with more precise observational data would probably improve future simulations. On the other hand, our results are not significantly affected by the choice of CTD or reanalysis data when defining the initial ocean temperature and salinity profiles. This suggests that accurate process-based models and observational constraints on submarine melt and calving are more important when making projections about future response of Greenland outlet glaciers to climate change. Additional uncertainty related to dynamic parameters and topography data (bedrock, width) are not included in this study.

Overall, we obtain a total Greenland glaciers SLR contribution of approximately ~~5 cm~~ 50 mm when assuming a linear relationship between the glacier's present-day grounding line discharge and their contribution to future SLR. Our estimate for SLR is lower than in Nick et al. (2013) (~~6.5-18.3cm~~65-183 mm) partly due to the fact that we took into consideration also smaller marine terminating glaciers. As Goelzer et al. (2013) argues, these glaciers probably become land-terminating faster than glaciers with a large grounding line discharge and have less mass influenced by ice-ocean interaction. Therefore our upscaling method for the strong climate change scenario should not be used past the year 2100. Furthermore, we demonstrate the sensitivity of the upscaling method to the choice and number of glaciers: by using only 4 glaciers as in Nick et al. (2013), the different choice of glaciers leads to uncertainty ranges of 15-80mm SLR.

Our simulations considered a constant catchment area for each glacier and did not account for potential changes in lateral inflow from the ice sheet interior. Such increased mass inflow could result in a smaller grounding line retreat but an increased inflow would also result in a broadening of the catchment area, as Goelzer et al. (2013) indicate, which could increase ice sheet mass loss further upstream. The full impact can only be assessed with experiments in which outlet glaciers and the parent ice sheet are fully coupled. Additionally, the 1D flowline model ~~treat~~ treats lateral processes in a simplified manner, so that more complex bedrock geometries (e.g. branching of glaciers, individual sills, unsymmetrical valley forms) are poorly represented in these estimations. For a first approximation, though, we treat the SLR of 5 cm as additional to that simulated with coarse resolution GrIS ice-sheet models, since the cumulative SMB forcing (without glacier response) over the glaciers' area is negligible. Some inconsistency arises from the fact that the database used to initialize the glaciers at the year 2000 ~~are~~ is actually based on the measurements made in 2008/2009, but the total contribution of GrIS to global seal level rise during the first 8 years of the 21st century was only about 3 mm and glaciers contributed not more than half of that. Thus this inconsistency has only a minor effect on our moderate approximation of ~~5 cm~~50 mm.

By adding the 5 cm contribution of outlet glaciers to the 8.8 cm (mid-range scenario) simulated by Calov et al. (2018) for the year 2100 using an ice sheet model under the same climate scenario, we arrive at a total GrIS contribution ~~13.8 cm (10.3 -16.8 cm~~ 138 mm (103 -168 mm from lower sample size range).

This implies that the dynamical response of Greenland's outlet glaciers to climate change can increase GrIS contribution to SLR in 2100 by over 50 %.

Author contributions. J.B designed the study together with A. G.. M.P. wrote the glacier model in FORTRAN and provided 1D topography data for the 12 glaciers of this study. J.B. coupled the numerical plume model to the glacier model, and implemented the surface-correction method. Together with S.B, R.C and M.W, J.B. created the projected subglacial discharge and surface-mass balance data set for each glacier respectively. J.B. carried out the experiments, created the figures and wrote the manuscript, supported by all co-authors.

Competing interests. The authors declare no competing interests.

Acknowledgements. This work was funded by Leibniz-Gemeinschaft, WGL Pakt für Forschung SAW-2014-PIK-1. M. W. and R. C. acknowledge support by the BMBF funded project PalMod.

References

Amundson, J. M. and Carroll, D.: Effect of Topography on Subglacial Discharge and Submarine Melting During Tidewater Glacier Retreat, Journal of Geophysical Research: Earth Surface, 123, 66–79, https://doi.org/10.1002/2017JF004376, http://doi.wiley.com/10.1002/2017JF004376, 2018.

Aschwanden, A., Fahnestock, M. A., and Truffer, M.: Complex Greenland outlet glacier flow captured, Nature Communications, 7, 10 524, 2016.

Bamber, J. L., Griggs, J. a., Hurkmans, R. T. W. L., Dowdeswell, J. a., Gogineni, S. P., Howat, I., Mouginot, J., Paden, J., Palmer, S., Rignot, E., and Steinhage, D.: A new bed elevation dataset for Greenland, Cryosphere, 7, 499–510, https://doi.org/10.5194/tc-7-499-2013, 2013.

Beckmann, J., Perrette, M., and Ganopolski, A.: Simple models for the simulation of submarine melt for a Greenland glacial system model, Cryosphere, 12, 301–323, https://doi.org/10.5194/tc-12-301-2018, 2018.

Benn, D. I., Aström, J., Zwinger, T., Todd, J., Nick, F. M., Cook, S., Hulton, N. R., and Luckman, A.: Melt-under-cutting and buoyancy-driven calving from tidewater glaciers: New insights from discrete element and continuum model simulations, Journal of Glaciology, 63, 691–702, https://doi.org/10.1017/jog.2017.41, 2017.

Bevan, S. L., Luckman, a. J., and Murray, T.: Glacier dynamics over the last quarter of a century at Helheim, Kangerdlugssuaq and 14 other major Greenland outlet glaciers, The Cryosphere, 6, 923–937, https://doi.org/10.5194/tc-6-923-2012, http://www.the-cryosphere.net/6/923/2012/, 2012.

Bondzio, J. H., Morlighem, M., Seroussi, H., Kleiner, T., Rückamp, M., Mouginot, J., Moon, T., Larour, E. Y., and Humbert, A.: The mechanisms behind Jakobshavn Isbræ's acceleration and mass loss: A 3-D thermomechanical model study, Geophysical Research Letters, 44, 6252–6260, https://doi.org/10.1002/2017GL073309, 2017.

Calov, R., Beyer, S., Greve, R., Beckmann, J., Willeit, M., Kleiner, T., Rückamp, M., Humbert, A., and Ganopolski, A.: Simulation of the future sea level contribution of Greenland with a new glacial system model, The Cryosphere Discussions, 2018, 1–37, https://doi.org/10.5194/tc-2018-23, https://www.the-cryosphere-discuss.net/tc-2018-23/, 2018.

Carroll, D., Sutherland, D. a., Shroyer, E. L., Nash, J. D., Catania, G. a., and Stearns, L. a.: Modeling Turbulent Subglacial Meltwater Plumes: Implications for Fjord-Scale Buoyancy-Driven Circulation, Journal of Physical Oceanography, p. In press, https://doi.org/10.1175/JPO-D-15-0033.1, http://journals.ametsoc.org/doi/abs/10.1175/JPO-D-15-0033.1, 2015.

Chen, X., Zhang, X., Church, J. A., Watson, C. S., King, M. A., Monselesan, D., Legresy, B., and Harig, C.: The increasing rate of global mean sea-level rise during 1993-2014, Nature Climate Change, 7, 492–495, https://doi.org/10.1038/nclimate3325, http://dx.doi.org/10.1038/nclimate3325{%}0Ahttp://10.0.4.14/nclimate3325{%}0Ahttp://www.nature.com/nclimate/journal/vaop/ncurrent/abs/nclimate3325.html{#}supplementary-information{%}5Cnhttp://www.nature.com/doifinder/10.1038/nclimate3325, 2017.

Cowton, T., Slater, D., Sole, A., Goldberg, D., and Nienow, P.: Modeling the impact of glacial runoff on fjord circulation and submarine melt rate using a new subgrid-scale parameterization for glacial plumes, Journal of Geophysical Research: Oceans, 120, 796–812, https://doi.org/10.1002/2014JC010324, 2015.

Dowdeswell, J. A., Evans, J., and Cofaigh, C. Ó.: Submarine landforms and shallow acoustic stratigraphy of a 400 km-long fjord-shelf-slope transect, Kangerlussuaq margin, East Greenland, Quaternary Science Reviews, 29, 3359–3369, https://doi.org/10.1016/j.quascirev.2010.06.006, http://dx.doi.org/10.1016/j.quascirev.2010.06.006, 2010.

Enderlin, E. M. and Howat, I. M.: Submarine melt rate estimates for floating termini of Greenland outlet glaciers (2000–2010), Journal of Glaciology, 59, 67–75, https://doi.org/10.3189/2013JoG12J049, http://openurl.ingenta.com/content/xref?genre=article{&}issn=0022-1430{&}volume=59{&}issue=213{&}spage=67, 2013.

Enderlin, E. M., Howat, I. M., and Vieli, A.: High sensitivity of tidewater outlet glacier dynamics to shape, The Cryosphere, 7, 1007–1015, https://doi.org/10.5194/tc-7-1007-2013, http://www.the-cryosphere.net/7/1007/2013/, 2013.

Enderlin, E. M., Howat, I. M., Jeong, S., Noh, M. J., Van Angelen, J. H., and Van Den Broeke, M. R.: An improved mass budget for the Greenland ice sheet, Geophysical Research Letters, 41, 866–872, https://doi.org/10.1002/2013GL059010, 2014.

Fettweis, X., Franco, B., Tedesco, M., Van Angelen, J. H., Lenaerts, J. T., Van Den Broeke, M. R., and Gallée, H.: Estimating the Greenland ice sheet surface mass balance contribution to future sea level rise using the regional atmospheric climate model MAR, Cryosphere, 7, 469–489, https://doi.org/10.5194/tc-7-469-2013, 2013.

Fried, M. J., Catania, G. A., Bartholomaus, T. C., Duncan, D., Davis, M., Stearns, L. A., Nash, J., Shroyer, E., and Sutherland, D.: Distributed subglacial discharge drives significant submarine melt at a Greenland tidewater glacier, pp. 4–7, 2015.

Fürst, J. J., Goelzer, H., and Huybrechts, P.: Ice-dynamic projections of the Greenland ice sheet in response to atmospheric and oceanic warming, The Cryosphere, 9, 1039–1062, https://doi.org/10.5194/tcd-8-3851-2014, http://www.the-cryosphere-discuss.net/8/3851/2014/, 2015.

Gillet-Chaulet, F., Gagliardini, O., Seddik, H., Nodet, M., Durand, G., Ritz, C., Zwinger, T., Greve, R., and Vaughan, D. G.: Greenland ice sheet contribution to sea-level rise from a new-generation ice-sheet model, Cryosphere, 6, 1561–1576, https://doi.org/10.5194/tc-6-1561-2012, 2012.

Goelzer, H., Huybrechts, P., Fürst, J., Nick, F., Andersen, M., Edwards, T., Fettweis, X., a.J. Payne, and Shannon, S.: Sensitivity of Greenland ice sheet projections to model formulations, Journal of Glaciology, 59, 733–749, https://doi.org/10.3189/2013JoG12J182, http://www.igsoc.org/journal/59/216/j12J182.html, 2013.

Goelzer, H., Robinson, A., Seroussi, H., and van de Wal, R. S.: Recent Progress in Greenland Ice Sheet Modelling, Current Climate Change Reports, 3, 291–302, https://doi.org/10.1007/s40641-017-0073-y, http://link.springer.com/10.1007/s40641-017-0073-y, 2017.

Helsen, M. M., van de Wal, R. S. W., van den Broeke, M. R., van de Berg, W. J., and Oerlemans, J.: Coupling of climate models and ice sheet models by surface mass balance gradients: application to the {Greenland} Ice Sheet, The Cryosphere, 6, 255–272, https://doi.org/doi:10.5194/tc-6-255-2012, 2012, 2012.

Inall, M. E., Murray, T., Cottier, F. R., Scharrer, K., and Boyd, T. J.: Oceanic heat delivery via Kangerdlugssuaq Fjord to the south-east Greenland ice sheet, Journal of Geophysical Research : Oceans, pp. 631–645, https://doi.org/10.1002/2013JC009295.Received, 2014.

Jackson, R. H., Straneo, F., and Sutherland, D. A.: Externally forced fluctuations in ocean temperature at Greenland glaciers in non-summer months, Nature Geoscience, 7, 503–508, https://doi.org/10.1038/ngeo2186, http://www.nature.com/ngeo/journal/v7/n7/full/ngeo2186.html?WT.ec{_}id=NGEO-201407, 2014.

Jackson, R. H., Shroyer, E. L., Nash, J. D., Sutherland, D. A., Carroll, D., Fried, M. J., Catania, G. A., Bartholomaus, T. C., and Stearns, L. A.: Near-glacier surveying of a subglacial discharge plume: implications for plume parameterizations, Geophysical Research Letters, https://doi.org/10.1002/2017GL073602, http://doi.wiley.com/10.1002/2017GL073602, 2017.

Jenkins, A.: Convection-Driven Melting near the Grounding Lines of Ice Shelves and Tidewater Glaciers, Journal of Physical Oceanography, 41, 2279–2294, https://doi.org/10.1175/JPO-D-11-03.1, http://journals.ametsoc.org/doi/abs/10.1175/JPO-D-11-03.1, 2011.

Khan, S. a., Kjaer, K. H., Bevis, M., Bamber, J. L., Wahr, J., Kjeldsen, K. K., Bjork, A. a., Korsgaard, N. J., Stearns, L. a., van den Broeke, M. R., Liu, L., Larsen, N. K., and Muresan, I. S.: Sustained mass loss of the northeast Greenland ice sheet triggered by regional warming, Nature Clim. Change, 4, 292–299, https://doi.org/10.1038/nclimate2161, http://dx.doi.org/10.1038/nclimate2161{%}5Cn10.1038/nclimate2161{%}5Cnhttp://www.nature.com/nclimate/journal/v4/n4/abs/nclimate2161.html{#}supplementary-information, 2014.

Lindbäck, K., Pettersson, R., Hubbard, A. L., Doyle, S. H., Van As, D., Mikkelsen, A. B., and Fitzpatrick, A. A.: Subglacial water drainage, storage, and piracy beneath the Greenland ice sheet, Geophysical Research Letters, 42, 7606–7614, https://doi.org/10.1002/2015GL065393, 2015.

Moon, T., Joughin, I., Smith, B., and Howat, I.: 21st-Century Evolution of Greenland Outlet Glacier Velocities, Science, 336, 576–578, 2012.

Morlighem, M., Rignot, E., Mouginot, J., Seroussi, H., and Larour, E.: Deeply incised submarine glacial valleys beneath the Greenland ice sheet, Nature Geoscience, 7, 418–422, https://doi.org/10.1038/ngeo2167, http://www.nature.com/doifinder/10.1038/ngeo2167, 2014.

Mortensen, J., Bendtsen, J., Motyka, R. J., Lennert, K., Truffer, M., Fahnestock, M., and Rysgaard, S.: On the seasonal freshwater stratification in the proximity of fast-flowing tidewater outlet glaciers in a sub-Arctic sill fjord, Journal of Geophysical Research: Oceans, 118, 1382–1395, https://doi.org/10.1002/jgrc.20134, 2013.

Muresan, I. S. and Khan, S. A.: Modelling dynamics of Jakobshavn Isbr{æ} and its contribution to sea level rise over the past and future century, Danmarks Tekniske Universitet (DTU), 2016.

Nick, F., van der Veen, C., Vieli, a., and Benn, D.: A physically based calving model applied to marine outlet glaciers and implications for the glacier dynamics, Journal of Glaciology, 56, 781–794, https://doi.org/10.3189/002214310794457344, http://openurl.ingenta.com/content/xref?genre=article{&}issn=0022-1430{&}volume=56{&}issue=199{&}spage=781, 2010.

Nick, F. M., Vieli, A., Andersen, M. L., Joughin, I., Payne, A., Edwards, T. L., Pattyn, F., and van de Wal, R. S. W.: Future sea-level rise from Greenland's main outlet glaciers in a warming climate, Nature, 497, 235–238, https://doi.org/10.1038/nature12068, http://www.nature.com/doifinder/10.1038/nature12068, 2013.

Peano, D., Colleoni, F., Quiquet, A., and Masina, S.: Ice flux evolution in fast flowing areas of the {Greenland} ice sheet over the 20th and 21st centuries, J. Glaciol., 63, 499–513, https://doi.org/10.1017/jog.2017.12, 2017.

Rignot, E. and Mouginot, J.: Ice flow in Greenland for the International Polar Year 2008-2009, Geophys. Res. Lett., 39, L11 501, https://doi.org/10.1029/2012GL051634, 2012.

Rignot, E., Box, J. E., Burgess, E., and Hanna, E.: Mass balance of the {Greenland} ice sheet from 1958 to 2007, Geophys. Res. Lett., 35, L20 502, https://doi.org/10.1029/2008GL035417, 2008.

Rignot, E., Fenty, I., Xu, Y., Cai, C., and Kemp, C.: Undercutting of marine-terminating glaciers in West Greenland, Geophysical Research Letters, 42, 5909–5917, https://doi.org/10.1002/2015GL064236, 2015.

Rignot, E., Fenty, I., Xu, Y., Cai, C., Velicogna, I., Cofaigh, C., Dowdeswell, J. A., Weinrebe, W., Catania, G., and Duncan, D.: Bathymetry data reveal glaciers vulnerable to ice-ocean interaction in Uummannaq and Vaigat glacial fjords, west Greenland, Geophysical Research Letters, 43, 2667–2674, https://doi.org/10.1002/2016GL067832, 2016.

Schaffer, J., Timmermann, R., Erik Arndt, J., Savstrup Kristensen, S., Mayer, C., Morlighem, M., and Steinhage, D.: A global, high-resolution data set of ice sheet topography, cavity geometry, and ocean bathymetry, Earth System Science Data, 8, 543–557, https://doi.org/10.5194/essd-8-543-2016, 2016.

Schaffer, J., von Appen, W. J., Dodd, P. A., Hofstede, C., Mayer, C., de Steur, L., and Kanzow, T.: Warm water pathways toward Nioghalvfjerdsfjorden Glacier, Northeast Greenland, Journal of Geophysical Research: Oceans, 122, 4004–4020, https://doi.org/10.1002/2016JC012462, 2017.

Schoof, C., Davis, A. D., and Popa, T. V.: Boundary layer models for calving marine outlet glaciers, Cryosphere, 11, 2283–2303, https://doi.org/10.5194/tc-11-2283-2017, 2017.

Sciascia, R., Straneo, F., Cenedese, C., and Heimbach, P.: Seasonal variability of submarine melt rate and circulation in an East Greenland fjord, Journal of Geophysical Research: Oceans, 118, 2492–2506, https://doi.org/10.1002/jgrc.20142, http://doi.wiley.com/10.1002/jgrc.20142, 2013.

Seddik, H., Greve, R., Zwinger, T., Gillet-Chaulet, F., and Gagliardini, O.: Simulations of the Greenland ice sheet 100 years into the future with the full Stokes model Elmer/Ice, Journal of Glaciology, 58, 427–440, https://doi.org/10.3189/2012JoG11J177, http://www.igsoc.org/journal/58/209/t11J177.html, 2012.

Slater, D., Nienow, P., Sole, A., Cowton, T. O. M., Mottram, R., Langen, P., and Mair, D.: Spatially distributed runoff at the grounding line of a large Greenlandic tidewater glacier inferred from plume modelling, Journal of Glaciology, pp. 1–15, https://doi.org/10.1017/jog.2016.139, 2017.

Slater, D. A. and Straneo, F.: Localized Plumes Drive Front-Wide Ocean Melting of A Greenlandic Tidewater Glacier, pp. 350–358, https://doi.org/10.1029/2018GL080763, 2018.

Slater, D. A., Nienow, P. W., Cowton, T. R., Goldberg, D. N., and Sole, A. J.: Effect of near-terminus subglacial hydrology on tidewater glacier submarine melt rates, Geophysical Research Letters, 42, 2861–2868, https://doi.org/10.1002/2014GL062494, 2015.

Straneo, F. and Heimbach, P.: North Atlantic warming and the retreat of Greenland's outlet glaciers., Nature, 504, 36–43, https://doi.org/10.1038/nature12854, http://www.ncbi.nlm.nih.gov/pubmed/24305146, 2013.

Straneo, F., Sutherland, D. a., Holland, D., Gladish, C., Hamilton, G. S., Johnson, H. L., Rignot, E., Xu, Y., and Koppes, M.: Characteristics of ocean waters reaching greenland's glaciers, Annals of Glaciology, 53, 202–210, https://doi.org/10.3189/2012AoG60A059, 2012.

Straneo, F., Hamilton, G. S., Stearns, L. A., and Society, T. O.: Oceanography 29(4):34–45,, 2016.

Syvitski, J., Andrews, J., and Dowdeswell, J.: Sediment deposition in an iceberg-dominated glacimarine environment, East Greenland: basin fill implications, Global and Planetary Change, 12, 251–270, https://doi.org/10.1016/0921-8181(95)00023-2, 1996.

Vallot, D., Åström, J., Zwinger, T., Pettersson, R., Everett, A., Benn, D. I., Luckman, A., Van Pelt, W. J., Nick, F., and Kohler, J.: Effects of undercutting and sliding on calving: A global approach applied to Kronebreen, Svalbard, Cryosphere, 12, 609–625, https://doi.org/10.5194/tc-12-609-2018, 2018.

van den Broeke, M., Box, J., Fettweis, X., Hanna, E., Noël, B., Tedesco, M., van As, D., van de Berg, W. J., and van Kampenhout, L.: Greenland Ice Sheet Surface Mass Loss: Recent Developments in Observation and Modeling, Current Climate Change Reports, 3, 345–356, https://doi.org/10.1007/s40641-017-0084-8, http://link.springer.com/10.1007/s40641-017-0084-8, 2017.

Van Den Broeke, M. R., Enderlin, E. M., Howat, I. M., Kuipers Munneke, P., Noël, B. P., Jan Van De Berg, W., Van Meijgaard, E., and Wouters, B.: On the recent contribution of the Greenland ice sheet to sea level change, Cryosphere, 10, 1933–1946, https://doi.org/10.5194/tc-10-1933-2016, 2016.

Van Der Veen, C. J. and Whillans, I. M.: Model experixnents on the evolution and stability of ice streams, Annals of Glaciology, 23, 129–137, 1996.

Vaughan, D. G., Comiso, J. C., Allison, I., Carrasco, J., Kaser, G., Kwok, R., Mote, P., Murray, T., Paul, F., Ren, J., Rignot, E., Solomina, O., Steffen, K., and Zhang, T.: Observations: Cryosphere, Climate Change 2013: The Physical Science Basis. Contribution of Working Group I to the Fifth Assessment Report of the Intergovernmental Panel on Climate Change, pp. 317–382, https://doi.org/10.1017/CBO9781107415324.012, 2013.

Xie, J., Bertino, L., Knut, L., and Sakov, P.: Quality assessment of the TOPAZ4 reanalysis in the Arctic over the period 1991-2013, Ocean Science, 13, 123–144, https://doi.org/10.5194/os-13-123-2017, 2017.

Xu, Y., Rignot, E., Fenty, I., Menemenlis, D., and Flexas, M. M.: Subaqueous melting of Store Glacier, west Greenland from three-dimensional, high-resolution numerical modeling and ocean observations, Geophysical Research Letters, 40, 4648–4653, https://doi.org/10.1002/grl.50825, http://doi.wiley.com/10.1002/grl.50825, 2013.

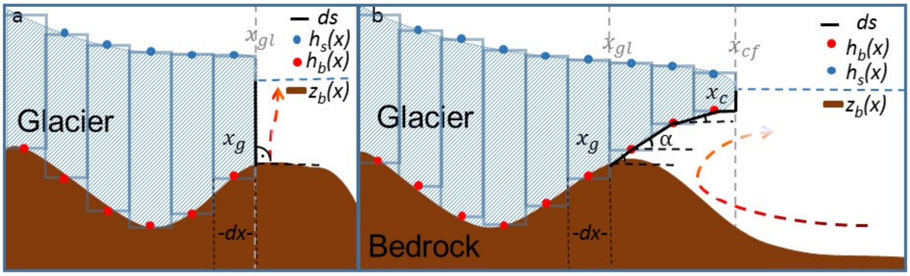

Figure 1. Visualiszation of the 1D glacier model with the staggered grid for a) a tidewater glacier and b) a glacier with a floating tongue. Red dots indicate where the depth of glacier base h_b is defined and blue dots where surface elevation h_s of the glacier is defined. They are calculated at dx/2 - the half width of each grid cell. Last grounded cell has the coordinate x_g and last floating cell has the coordinate x_c. The grounding line ~~gl_x~~ x_{gl} is determined at the border of the last grounded cell, where the flotation criterion is not yet achieved. After the grounding line, the calculation of submarine melt along the distance ds (thick, black line) is performed with the line plume model. For a floating tongue (b) every grid cell may have a different angle for the slope of glacial base while for a tidewater glacier (a) the angle is set to 90 degrees. The bedrock elevation z_b (brown, thick line) is equal to h_b for the grounded part and is deeper for the floating part of the glacier.

~~a) Bathymetry around Kangerlussuaq glacier (red star indicates glacier terminus). Black dots indicate the location of the CTD measurements made in September 2004. Red, thick dots show the location of CTD profiles used for the submarine melt rate calculations in the text and are indicated as white dashed lines in panel b). Closest CTD. Grid indicates the resolution of the reanalysis data and grey shaded squares show which reanalysis data points have a depth of at least 400 m. b) Vertical temperature distribution as a function of the distance from the glacier terminus, obtained by interpolation of the CTD profiles. White dashed lines correspond to the position of the red-marked CTD positions in panel a and give for a subglacial discharge 50 m^3s^{-1} an average melt rate of 0.5, 0.6 and 3.6 m/d (from left to right).~~

~~Monthly (thin lines) and annual mean (thick lines) of ocean temperature from reanalysis data of the closest point to fjord of Jakobshavn-Isbrae that has a minimum depth of a) 200m b) 400m and c) 700m depth. Location of these points differ due to the different area coverages for the corresponding depths (700m is mostly outside of continental shelf). Black dots show CTD measurements at the same depth but inside or close to the fjord. Same as in Fig. **??** but for Store Glacier.~~

~~Bathymetry and bedrock data close to the terminus of Store Glacier (red star). The labels 200, 400 and 700 indicate were the detection points of the reanalysis data closest to the glacier with the depth of 200 m, 400 m and 700 m were located.~~

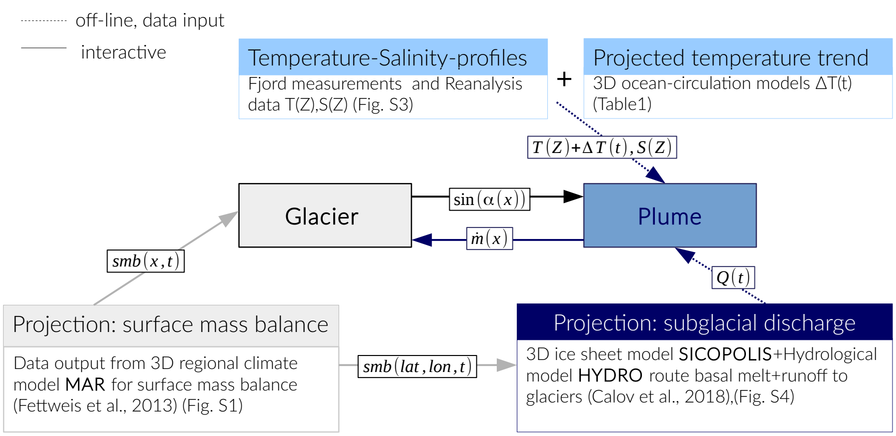

Figure 2. Visualisation of the experimental setup. In the center the coupled glacier-plume model exchange information on the glacier geometry ($\sin(\alpha)$) and the calculated submarine melt rate ($\dot{m}$) on every time step for every glacier grid-point x. To force the coupled model for global warming (RCP 8.5) changes in SMB ($smb(x,t)$), ocean temperature($T(Z)+\Delta T(t)$) and subglacial discharge ($Q(t)$) are considered via data-input. While the SMB changes act on the glacier part, the changes in subglacial discharge and ocean temperature are used to recalculate the submarine melt rate by the plume part of the model. The future evolution of subglacial discharge and ocean temperature is prescribed firmly in the data sets (off-line) that force the plume part, whereas changes in SMB are corrected for the surface elevation feedback and therefore regard changes in the ice surface height interactively. SMB is derived from MAR data (Fettweis et al., 2013), also used to derive the subglacial discharge for each glacier by Calov et al. (2018).

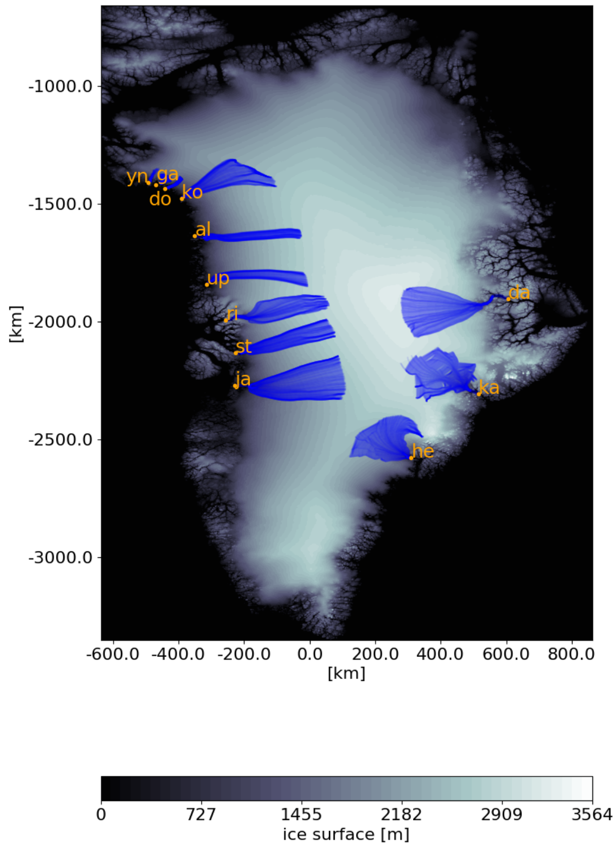

Figure 3. Terminus location (orange dot) with the catchment area (blue) of the twelve investigated glaciers: Alison Glacier (al), Daugaard-Jensen Glacier (da), Docker-Smith Glacier (do), Gade (ga) Helheim Glacier (he), Jakobshavn-Isbrae (ja), Kangerlussuaq Glacier (ka), Kong-Oscar Glacier (ko), Rink-Isbrae (ri), Store Glacier (st), Upernavik North Glacier (up), Yngvar-Nielsen Glacier (yn)

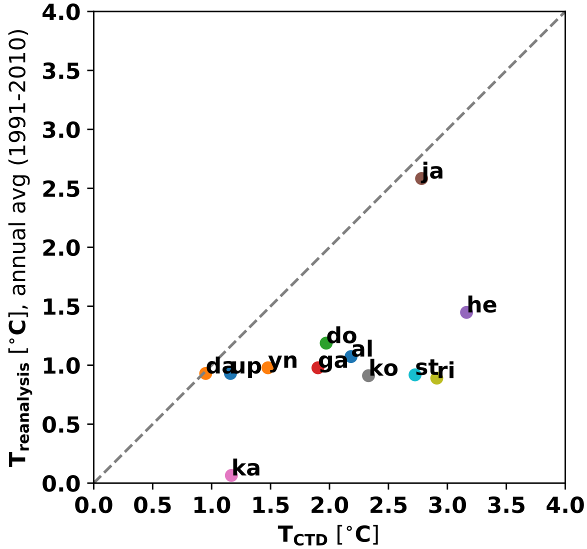

Figure 4. Temperature at the grounding line depth of CTD measurements closest to glacier front, inside the fjords (~~y-axis~~x-axis) and temperatures reconstructed from ~~Reanalysis~~ reanalysis data (y-axis) from the nearest possible grid-cell ~~with depth 400m averaged from 1991 -2010 (x-axis)~~ for all 12 glaciers: Alison (al), Daugaard-Jensen (da), Docker-Smith (do), Gade (ga), Helheim (he),Jakobshavn Isbrae (ji), Kangerlussuaq (ka), Kong Oscar (ko), Rink Isbrae (ri), Store (st), Upernavik (up), Yngvar Nielsen (yn).

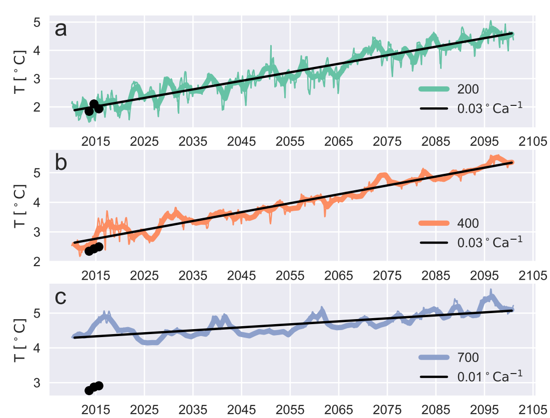

Figure 5. Monthly ocean temperature and centennial trend from the CMIP5 model MPI-ESM-LR in the closest grid-cells to the fjord of Rink Isbrae that have a depth of at least a) ~~200m~~ 200 m b) ~~400m~~ 400 m and c) ~~700m~~ 700 m depth. Black dots show CTD measurements at the same depth but inside the fjord.

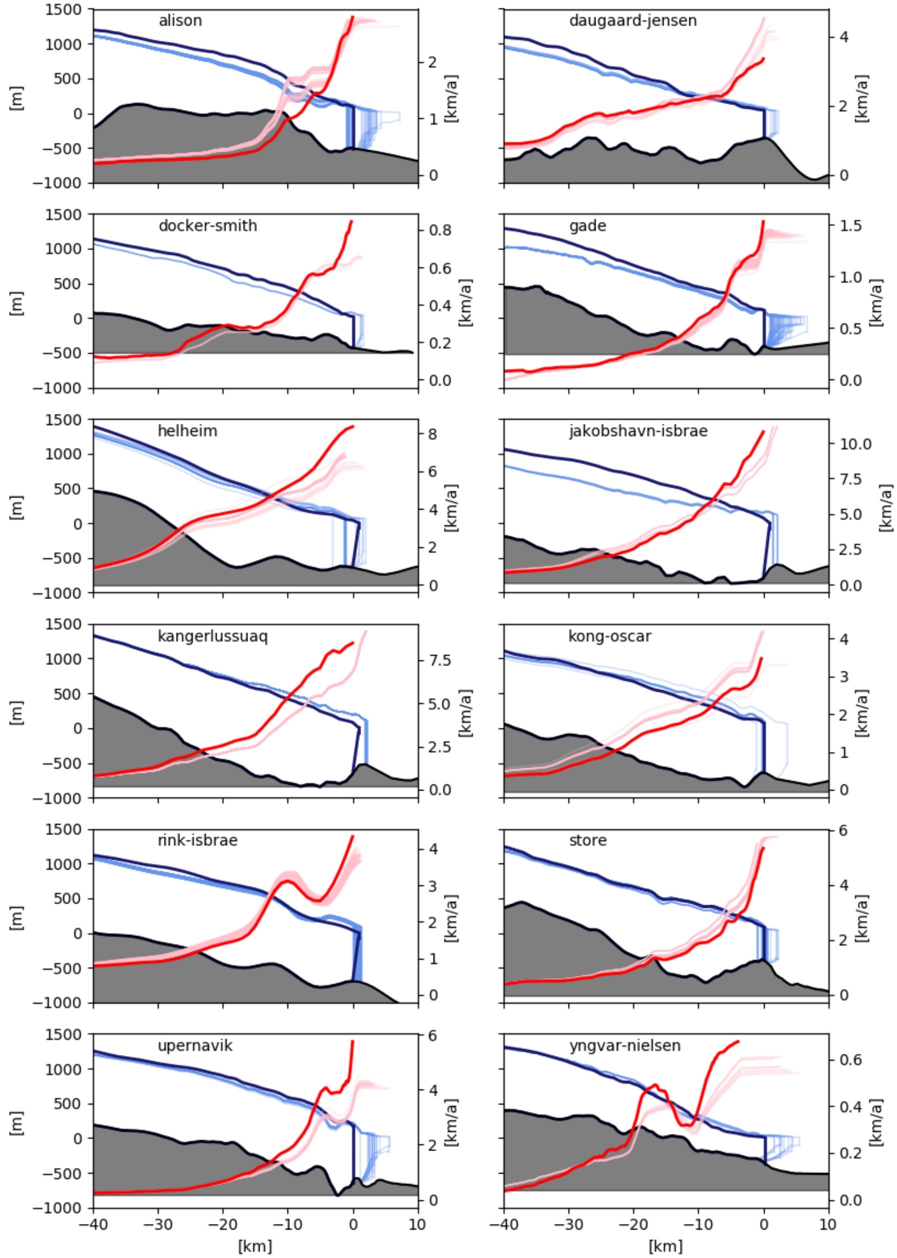

Figure 6. Simulated glacier elevation (light blue) and velocity profile (light red) for the last 40 km to the grounding line ~~plotted~~ depicted together with observational data (dark blue and dark red) by Morlighem et al. (2014) and Rignot and Mouginot (2012). Bedrock data is derived by the flux weighted average over the whole catchment area. ~~Number~~ The number of simulations is given in Tab. S3, supporting information

.

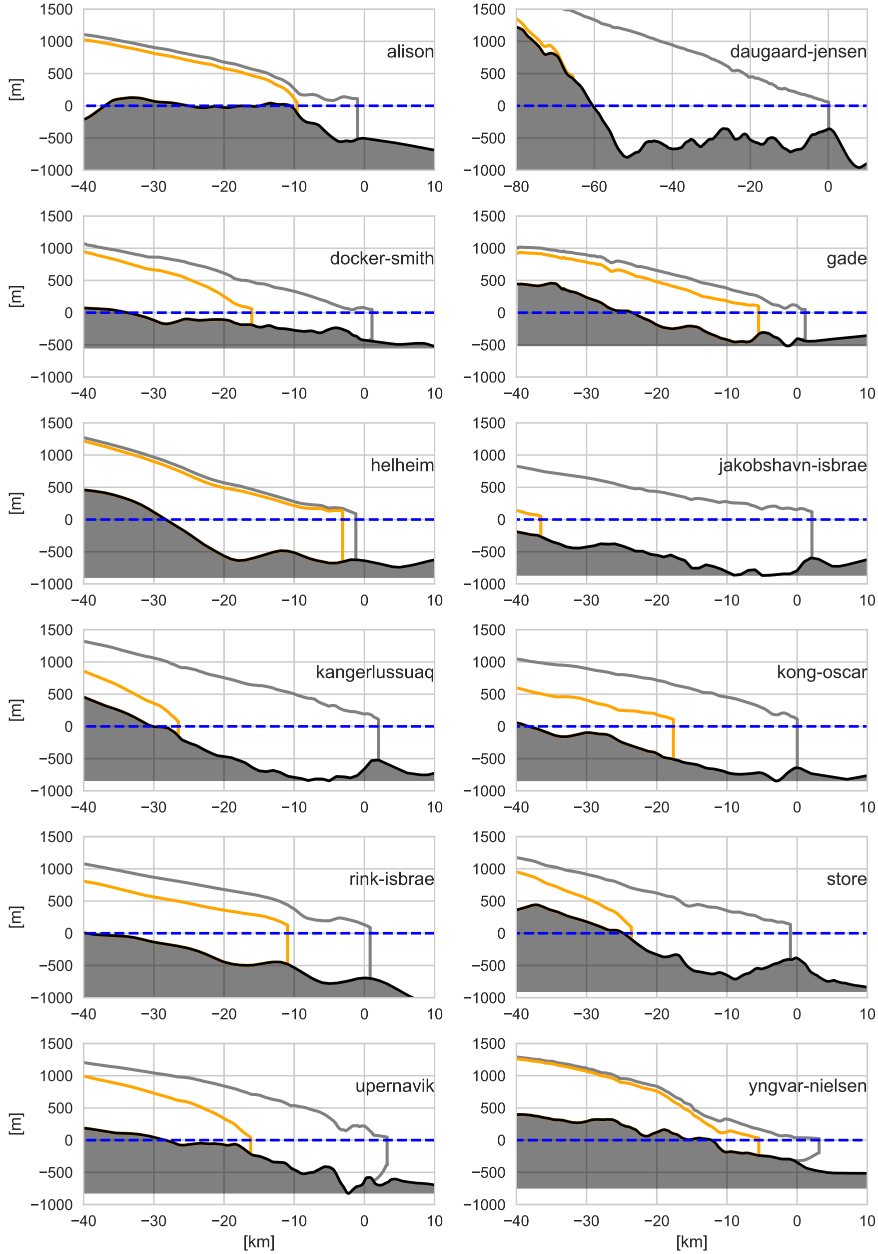

Figure 7. Retreat of median-range [3] SLR scenario for RCP 8.5 forcing scenarios (SMB and ocean temperature and subglacial discharge) for all 12 glaciers at 2100 (orange). Corresponding initial states are depicted in grey. Daugaard-Jensen, showed full retreat with over 80 km.

[3] median for an odd number of simulations, the first value of higher half for an even number of simulation

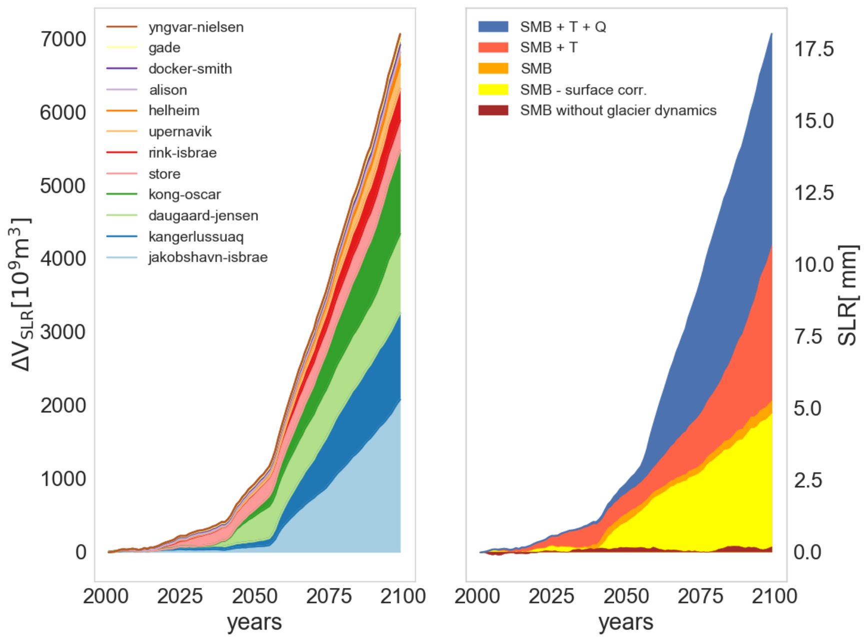

Figure 8. Cumulative sea level rise of median-range[3] SLR scenario from Fig. 7 for all 12 glaciers. Left panel: Individual glaciers' response to complete future forcing scenario (SMB, subglacial discharge Q and ocean temperature T in blue). Right panel: the The role of individual forcing factors for all glaciers. The dynamics response of all twelve glacier forced by $\mathrm{SMB+T+Q}$ (blue), $\mathrm{SMB+T}$ (pink), SMB forcing only (orange) and SMB without the surface elevation feedback in the glacier model (yellow). The 'static' cumulative SMB forcing from MAR is calculated anomaly over the whole fixed present-day catchment area of glacier domains and surface heights from MAR for all twelve glaciers (brown).

[3] median for an odd number of simulations, the first value of higher half for an even number of simulation

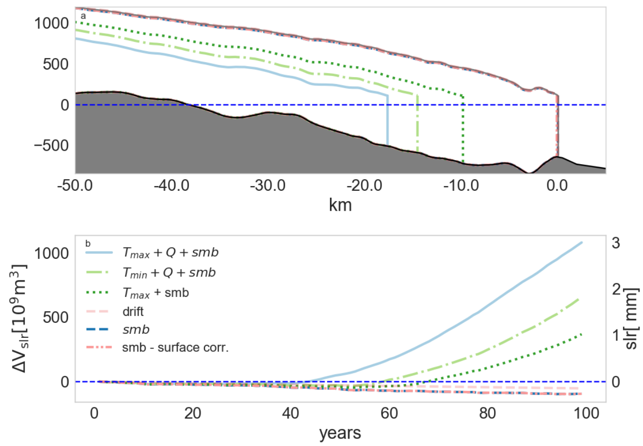

Figure 9. a) Kong-Oscar Glacier with a representative medium-slr retreat scenario applying forcing factors as subglacial discharge Q, ocean temperature T, surface mass balance smb with and without accounting for surface elevation correction (smb - surface corr.) for the medium SLR scenario. The corresponding SLR of each experiment is displayed in panel b).

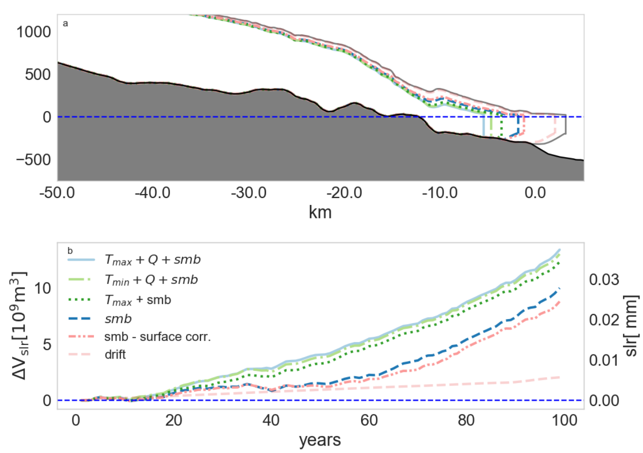

Figure 10. a) Yngvar Nielsen Glacier with a representative medium-slr retreat scenario applying forcing factors as subglacial discharge Q, ocean temperature T, surface mass balance smb with and without accounting for surface elevation correction (smb - surface corr.) for the medium SLR scenario. The corresponding SLR of each experiment is displayed in panel b).

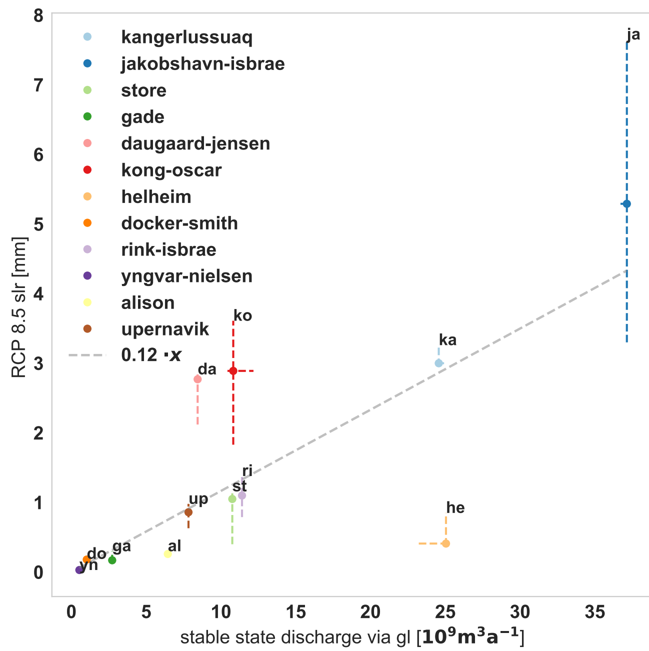

Figure 11. First to third quartile (median indicated with a dot) of contribution to SLR at 2100 under RCP 8.5 for each glacier from Table 3 as a function of the present-day grounding line discharge. The future simulations were forced by changes in SMB, subglacial discharge and minimal and maximal ocean temperature trend (Tab. 1). Grey dashed line , indicates a linear regression obtained with an ordinary least square method from the median values. Slope and p-value are $0.1\ \mathrm{mm\ km^{-3}\ a}$ and $9 \cdot 10^{-5}$, respectively. The correlation coefficient is 0.75 0.74.

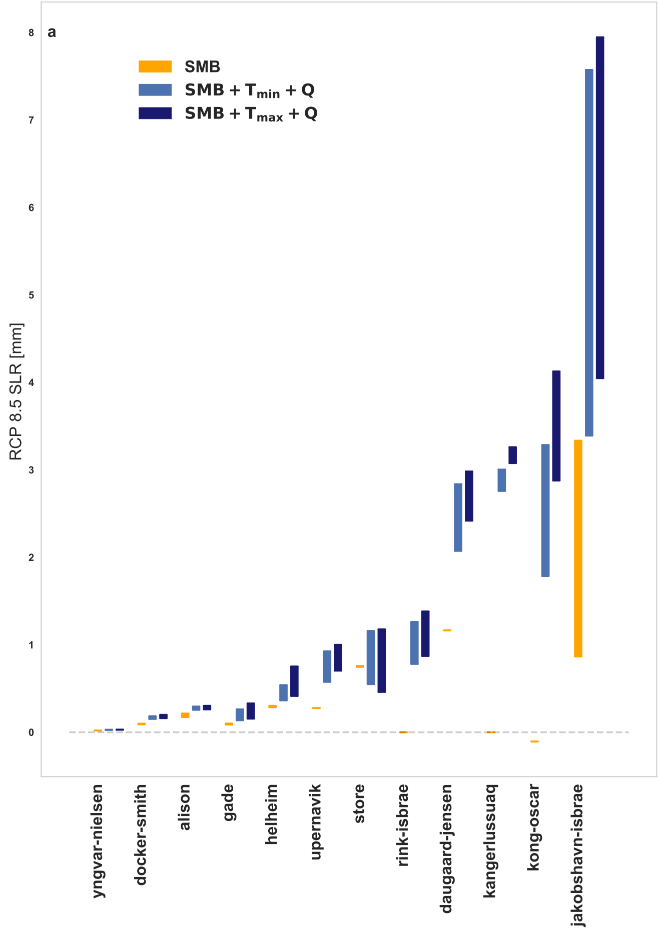

Figure 12. First to third quartile of contribution to SLR for each glacier. Future RCP 8.5 scenarios were either forced with SMB changes only (orange) or changes in SMB, ocean temperature (T_{min} and T_{max}) and subglacial discharge (blue).

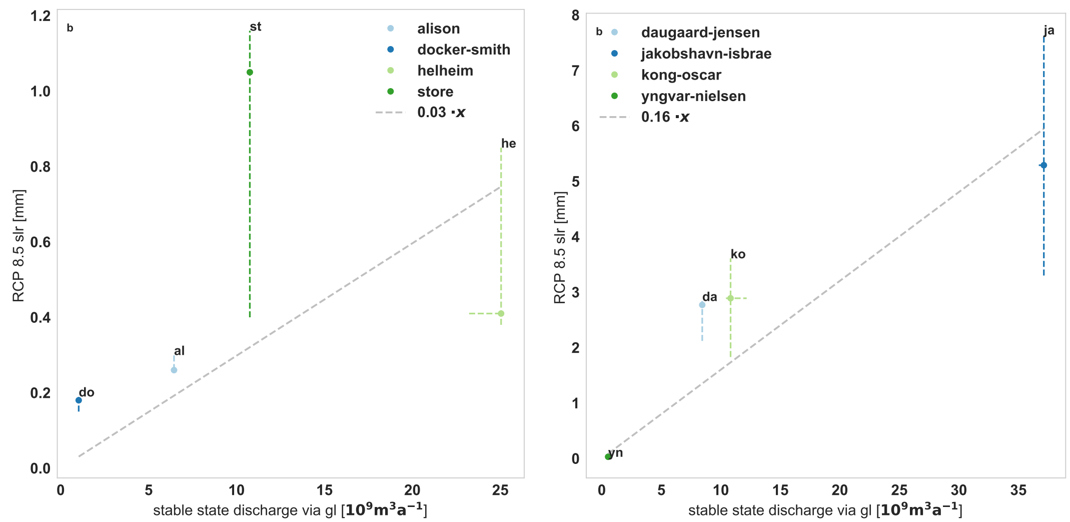

Figure 13. First to third quartile (median indicated with a dot) of contribution to SLR under RCP 8.5 for each glacier from Table 3 as a function of the present-day grounding line discharge. The future simulations were forced by changes in SMB, subglacial discharge and minimal and maximal ocean temperature trend (Tab. 1). Grey dashed line indicates a linear function of the present-day grounding line discharge in future SLR for 2100 obtained with an ordinary least square model from the median values for 4 glaciers only. For panel a slope and p-value are $0.03\ \mathrm{mm\ km^{-3}}$ a and 0.18 respectively, and for panel b $0.16\ \mathrm{mm\ km^{-3}}$ a and 0.01.

Table 1. Minimal and maximal ocean temperature trend over 100 years for three CMIP5 Models derived from the grid-cells closest to each glacier fjord with minimum 400m depth. Detailed information are listed in ~~table~~ Table S1, supporting information.

glacier name	$\Delta T_{\mathrm{min}}(^{\circ}\mathrm{C}/100\mathrm{a})$	$\Delta T_{\mathrm{max}}(^{\circ}\mathrm{C}/100\mathrm{a})$
Daugaard-Jensen	3	5
Helheim Glacier	2	3
Jakobshavn Isbae	2	4
Kangerlussuaq Glacier	3	4
Rink Isbrae	1	3
Store Glacier	1	3
Kong Oscar Glacier	1	3
Alison Glacier	1	3
Upernavik Isstrom	1	3
Yngvar Nielsen	1	3
Docker Smith Glacier	1	3
Gade Glacier	1	3

Table 2. Each investigated glacier with the mean grounding line discharge from observation $\mathrm{Flx}_{\mathrm{gl}}^{\star\mathrm{E}}$ (Enderlin and Howat, 2013) and from the stable state simulations $\mathrm{Flx}_{\mathrm{gl}}$ as well as the number of stable simulations (#). The melt flux range for floating termini from all present-day simulations $\mathrm{MeltFlx}$ and from the observational data $\mathrm{MeltFlx}^{\star\mathrm{E}}$ is calculated with the error ranges in Enderlin and Howat (2013) but with the condition $0 < \mathrm{MeltFlx}^{\star\mathrm{E}} < \mathrm{Flx}_{\mathrm{gl}}^{\star\mathrm{E}}$. The respective ratio of melt flux /grounding line discharge ($\mathrm{MeltFlx}/\mathrm{Flx}_{\mathrm{gl}}$) in % is listed ~~in~~ for the ~~last to columns~~simulation and observations ($^{\star E}$) and indicates how much ice that flows over the grounding line is lost by submarine melting. The sign * indicates glaciers for which the melt rate partition of the simulation does not overlap with the range of Enderlin and Howat (2013). Melt fluxes ~~of~~ are derived for floating ~~tongue~~ tongues and thus $\mathrm{MeltFlx} = 0$ indicates tidewater glaciers (no floating tongue). Store Glacier is not examined in Enderlin and Howat (2013).

glacier	$\mathrm{Flx}_{\mathrm{gl}}^{\star\mathrm{E}}$ 10^9 $[\mathrm{m}^3/\mathrm{a}]$	$\mathrm{Flx}_{\mathrm{gl}}$ 10^9 $[\mathrm{m}^3/\mathrm{a}]$	$\mathrm{MeltFlx}^{\star\mathrm{E}}$ 10^9 $[\mathrm{m}^3/\mathrm{a}]$	$\mathrm{MeltFlx}$ 10^9 $[\mathrm{m}^3/\mathrm{a}]$	$\mathrm{MeltFlx}^{\star\mathrm{E}}/\mathrm{Flx}_{\mathrm{gl}}^{\star\mathrm{E}}$ [%]	$\mathrm{MeltFlx}/\mathrm{Flx}_{\mathrm{gl}}$ [%]	#
alison	6.83	6.25 - 6.55	0.82 - 6.41	0.00 - 4.77	12 - 94	0 - 76	54
daugaard-jensen*	9.34	7.82 - 8.44	4.12 - 9.34	0.00 - 2.06	44 - 100	0 - 26	22
docker-smith	1.06	1.05 - 1.07	0.00 - 0.87	0.22 - 0.66	0 - 82	21 - 62	5
gade	4.85	2.63 - 2.81	0.00 - 4.85	0.17 - 2.14	0 - 100	6 - 77	55
helheim	29.16	22.84 - 25.94	0.19 - 6.90	0.00 - 8.39	1 - 24	0 - 36	28
jakobshavn-isbrae*	43.03	36.81 - 37.14	21.11 - 32.91	0.00 - 0.00	49 - 76	0 - 0	11
kangerlussuaq	38.80	24.51 - 24.58	0.00 - 6.83	0.00 - 0.00	0 - 18	0 - 0	39
kong-oscar	11.86	10.34 - 12.86	3.06 - 6.28	0.00 - 2.64	26 - 53	0 - 26	16
rink-isbrae	10.95	11.20 - 11.73	0.00 - 6.85	0.00 - 0.00	0 - 63	0 - 0	64
store	-	10.55 - 11.29	-	0.00 - 1.73	-	0 - 16	67
upernavik north	17.12	7.48 - 7.84	5.81 - 11.20	0.03 - 5.92	34 - 65	0 - 78	21
yngvar-nielsen	0.69	0.53 - 0.56	0.00 - 0.69	0.08 - 0.42	0 - 100	15 - 76	11

Table 3. Median, first and third quartile of SLR contribution from each glacier under RCP 8.5 scenario (SMB, subglacial discharge and ocean temperature (min and max)). Values are corrected from drift.~~Negative values in SLR indicate SMB gain.~~

	slr [mm]		
glacier	median	first quartile	third quartile
alison	0.26	0.26	0.30
daugaard-jensen	2.73	2.12	2.84
docker-smith	0.18	0.15	0.19
gade	0.17	0.14	0.30
helheim	0.41	0.38	0.85
kangerlussuaq	3.00	2.96	3.26
kong-oscar	2.89	1.83	3.61
rink-isbrae	1.10	0.79	1.38
store	1.05	0.40	1.16
upernavik	0.85	0.63	0.98
yngvar-nielsen	0.03	0.03	0.03
jakobshavn-isbrae	5.22	3.30	7.65
sum	17.90	12.99	22.55

Table 4. Median, first and third quartile of grounding line retreat from each glacier under RCP 8.5 scenario (SMB, subglacial discharge and ocean temperature (min and max)). Values are corrected from drift.

	grounding line retreat [km]		
glacier	median	first quartile	third quartile
alison	9.21	8.69	10.77
daugaard-jensen	60.80	28.99	62.21
docker-smith	15.13	14.23	16.49
gade	5.85	4.62	15.17
helheim	1.52	1.10	9.63
kangerlussuaq	28.52	28.44	28.53
kong-oscar	17.65	14.61	18.63
rink-isbrae	11.07	10.90	11.18
store	17.59	3.99	23.21
upernavik	17.43	12.79	17.72
yngvar-nielsen	4.69	4.28	5.22
jakobshavn-isbrae	38.57	19.85	40.53
avg	19.00	12.71	21.61